

# **Fragility analysis of Masonry Infilled Reinforced Concrete building by Coefficient based method**

*A Thesis Submitted in Partial Fulfillment of the Requirements for  
the Degree of*

**MASTER OF TECHNOLOGY  
IN  
CIVIL ENGINEERING**



**JYOTI PRAKASH DASH**

**DEPARTMENT OF CIVIL ENGINEERING  
NATIONAL INSTITUTE OF TECHNOLOGY, ROURKELA  
2015**

# FRAGILITY ANALYSIS OF MASONRY INFILLED REINFORCED CONCRETE BUILDING BY COEFFICIENT BASED METHOD

*A Thesis Submitted in Partial Fulfillment of the Requirements for  
the Degree of*

*Master of Technology  
In  
Civil Engineering  
(Specialization: Structural Engineering)*

*Submitted By:*

**JYOTI PRAKASH DASH  
(ROLL NO. 213CE2061)**

***Under the guidance and supervision of  
Prof. Robin Davis P***



**DEPARTMENT OF CIVIL ENGINEERING  
NATIONAL INSTITUTE OF TECHNOLOGY, ROURKELA  
2015**



Department of Civil Engineering  
National Institute of Technology, Rourkela

## CERTIFICATE

---

This is to certify that the project entitled, “*Fragility analysis of masonry in-filled reinforced concrete building by Coefficient based method*” submitted by **Jyoti Prakash Dash** in “*Structural Engineering*” specialization is an authentic work carried out by him under my supervision and guidance for the partial fulfilment of the requirements for the award of **Master of Technology in Civil Engineering** during the academic session **2014-2015** at **National Institute of Technology, Rourkela**. The candidate has fulfilled all the prescribed requirements. The Thesis which is based on candidate’s own work, has not been submitted elsewhere for any degree. In my opinion, the thesis is of standard requirement for the award of a Master of Technology in Civil Engineering.

×

---

Date:  
Place:

Dr. Robin Davis P  
Dept. of Civil Engineering.

# ACKNOWLEDGEMENT

---

Firstly, I am grateful to the Department of Civil Engineering, for giving me the opportunity to carry out this project, which is an integral fragment of the curriculum in M. Tech programme at the National Institute of Technology, Rourkela.

I would like to express my heartfelt gratitude and regards to my project guide, Prof. Robin Davis P, for being the corner stone of my project. It was his incessant motivation and guidance during periods of doubts and uncertainties that has helped me to carry on with this project. I would also like to thank Prof. S. K. Sahu, Head of the Department, Civil Engineering, for his guidance and support.

I would also like to thank a lot of other friends for giving a patient ear to my problems. I am also obliged to the staff of Civil Engineering for aiding me during the course of our project.

Finally, I would like to take the opportunity to thank my parents and my brother for their constant support and encouragement during my entire Post Graduate programme.

JYOTI PRAKASH DASH  
213CE2061

---

*Dedicated to my beloved family*

---

# ABSTRACT

---

Masonry infill Reinforced concrete frames are the most common type of structures used for multistorey constructions in the developing countries. Masonry infills, are the non-structural element, but provides resistance to the earthquake and prevent collapse of relatively flexible and weak RC structures. Seismic vulnerability of this type of structure has been studied in the earthquake ground motion.

Present study focuses on the seismic fragility analysis of masonry in-filled (MI) reinforced concrete (RC) buildings using coefficient based method. The coefficient-based method, is a simplified procedure without finite element analysis, for assessing spectral acceleration demand (or capacity) of buildings subjected to earthquakes. This paper begins with validation study of the proposed coefficient-based method for masonry infilled (MI) reinforced concrete (RC) buildings. Two, four and six storey masonry infilled (MI) reinforced concrete (RC) buildings are designed considering a bare frame analysis, to estimates the inter-storey drift demand and periodic shift factor in response to the peak ground for different set of ground motions. Using coefficient based method both spectral acceleration and spectral displacement-based fragility curves under various damage states (in terms of IDR) were then constructed.

Fragility curves obtained from the coefficient based method is compared with the SAC FEMA method at the collapse state and are correspondence well. The fragility curves obtained using both the method can provide a satisfactory vulnerability assessment for masonry infilled reinforced concrete (RC) buildings under different prescribed damage states (or performance level).

**Keywords:** MI RC building, drift factor, inter storey drift limit (IDR), periodic shift factor (PSF), peak ground acceleration (PGA), probabilistic seismic demand model (PSDM), fragility curves.

# TABLE OF CONTENTS

---

<b>Title</b>	<b>Page No.</b>
<b>ACKNOWLEDGEMENTS</b>	i
<b>ABSTRACT</b>	iii
<b>TABLE OF CONTENTS</b>	v
<b>LIST OF TABLES</b>	ix
<b>LIST OF FIGURES</b>	x
<b>ABBREVIATIONS</b>	xiii
<b>NOTATIONS</b>	xvi
<b>CHAPTER 1 INTRODUCTION</b>	1-6
1.1 Masonry infilled frames	1
1.2 Fragility curves	3
1.3 Background and Motivation	3
1.4 Research Objectives	4
1.5 Scope of the study	5



1.6 Methodology	5
1.7 Organization of thesis	6
<b>CHAPTER 2 LITERATURE REVIEW &amp; VALIDATION</b>	<b>7-31</b>
2.1 Introduction	7
2.2 Definition	8
2.2.1 Intensity measures	8
2.2.2 Building performance levels	9
2.2.3 Seismic fragility function methods	10
2.3 Review of previous studies on Analytical method	13
2.4 Methodology	17
2.4.1 Coefficient based method	17
2.4.2 Step wise procedure for Coefficient-based method	23
2.4.3 SAC FEMA method	24
2.5 Validation study of the coefficient based method	26
2.5.1 Spectral acceleration ( $S_a$ ) based fragility curve	26
2.5.2 Spectral displacement ( $S_d$ ) based fragility curve	29

2.6 Summary	31
<b>CHAPTER 3 DEVELOPMENT OF FRAGILITY CURVES</b>	<b>32-53</b>
3.1 Introduction	32
3.2 Methodology	32
3.3 Earthquake ground motion data	33
3.4 Fragility curves using Coefficient based method	35
3.4.1 Two storey building	35
3.4.2 Four storey building	38
3.4.3 Six storey building	41
3.4.4 Spectral acceleration ( $S_a$ ) based fragility curve by coefficient based method	44
3.4.5 Spectral displacement ( $S_d$ ) based fragility curve by coefficient based method	48
3.4.6 Comparison of fragility curve by coefficient based method and SAC FEMA method at the collapse state	51
3.5 Summary	53
<b>CHAPTER 4 CONCLUSIONS</b>	<b>54-57</b>
4.1 Summary	54

4.2 Concluding remarks	55
4.3 scope of future work	57
<b>REFERENCES</b>	58

## LIST OF TABLES

---

Table No.	Title	Page No.
3.1	Selected Indian Ground motion data.	34
3.2	Experimental data for 2-storey building.	35
3.3	Coefficient based parameters obtained from regression equation for 2-storey building.	38
3.4	Experimental data for 4-storey building.	38
3.5	Coefficient based parameters obtained from regression equation for 4-storey building.	41
3.6	Experimental data for 6-storey building.	41
3.7	Coefficient based parameters obtained from regression equation for 6-storey building.	44

# LIST OF FIGURES

---

Figure No.	Title	Page No.
1.1	Damage of MI RC building amid 2001 Bhuj Earthquake.	1
1.2	Change in lateral-load transfer mechanism due to masonry infills.	2
2.1	Spectral acceleration-based fragility curve by Özer & Erberik, 2008	15
2.2	Deformation model of a masonry in-filled reinforced concrete building.	20
2.3	Illustration of drift angle $\theta_{max}$ , $\theta_{lmax}$ , $\theta_{avg}$ .	21
2.4	Spectral acceleration based Fragility curves for two storey MI RC buildings	27
2.5	Spectral acceleration based Fragility curves for three storey MI RC buildings	27
2.6	Spectral acceleration based Fragility curves for four storey MI RC buildings	28
2.7	Spectral acceleration based Fragility curves for five storey MI RC buildings	28
2.8	Spectral displacement based Fragility curves for two storey MI RC buildings	29
2.9	Spectral displacement based Fragility curves for three storey MI RC buildings	29
2.10	Spectral displacement based Fragility curves for four storey MI RC buildings	30
2.11	Spectral displacement based Fragility curves for five storey MI RC buildings	30

3.1	Variation of Inter-storey drift ratio (IDR) with peak ground Acceleration (PGA) for 2-storey building.	36
3.2	Variation of Period shift factor (PSF) with peak ground Acceleration (PGA) for 2-storey building.	37
3.3	Variation of Inter-storey drift ratio (IDR) with peak ground Acceleration (PGA) for 4-storey building.	39
3.4	Variation of Period shift factor (PSF) with peak ground Acceleration (PGA) for 4-storey building.	40
3.5	Variation of Inter-storey drift ratio (IDR) with peak ground Acceleration (PGA) for 6-storey building.	42
3.6	Variation of Period shift factor (PSF) with peak ground Acceleration (PGA) for 6-storey building.	43
3.7	Spectral acceleration based fragility curve for two storey MI RC buildings.	45
3.8	Spectral acceleration based fragility curve for four storey MI RC buildings	45
3.9	Spectral acceleration based fragility curve for six storey MI RC buildings.	45
3.10	Spectral acceleration based fragility curve of MI RC buildings for various performance levels	46
3.11	spectral acceleration for two storey MI RC building corresponding to inter storey drift ratio of 0.005, 0.01 and 0.02	47
3.12	spectral acceleration for four storey MI RC building corresponding to inter storey drift ratio of 0.005, 0.01and 0.02	47
3.13	spectral acceleration for six storey MI RC building corresponding to inter storey drift ratio of 0.005, 0.01 and 0.02	48

3.14	Spectral displacement based fragility curve for two storey MI RC buildings for various performance level	48
3.15	Spectral displacement based fragility curve for four storey MI RC buildings for various performance level	49
3.16	Spectral displacement based fragility curve for six storey MI RC buildings for various performance level	49
3.17	spectral displacement for two storey MI RC building corresponding to inter storey drift ratio of 0.005, 0.01 and 0.02	50
3.18	spectral displacement for four storey MI RC building corresponding to inter storey drift ratio of 0.005, 0.01 and 0.02	50
3.19	spectral displacement for six storey MI RC building corresponding to inter storey drift ratio of 0.005, 0.01 and 0.02	51
3.20	Comparison of fragility curve of two storey MI RC buildings at the CP state (IDR=0.2%)	52
3.21	Comparison of fragility curve of four storey MI RC buildings at the CP state (IDR=0.2%)	52
3.22	Comparison of fragility curve of six storey MI RC buildings at the CP state (IDR=0.2%)	52

# ABBREVIATIONS

---

3-D	Three Dimensional
2-D	Two Dimensional
ASCE	American Society of Civil Engineers
ATC	Applied Technology Council
BF	Bare frame
C	Capacity
CESMD	Center for Engineering Strong Motion Data
CM	Confined Masonry
CP	Collapse Prevention
D	Demand
DF	Drift Factor
DOF	Degrees of Freedom
DPM	Damage Probability Matrices
EQ	Earthquake
EDP	Engineering Damage Parameter
FEM	Finite Element Method
FEMA	Federal Emergency Management Agency
FF	Fully in-filled frame
G	Ground



IDR	Inter-storey Drift Ratio
IM	Intensity Measure
IO	Immediate Occupancy
IS	Indian Standard
LS	Limit State
LS	Life Safety
MDOF	Multi Degree Of Freedom
MF	Multiplication Factor
MI	Masonry In-filled
NEHRP	National Earthquake Hazard Reduction Program
NTHA	Nonlinear Time History Analysis
NZSEE	New-Zealand Society for Earthquake Engineering
PGA	Peak Ground Acceleration
PGD	Permanent Ground Displacement
PGV	Peak Ground Velocity
POA	Pushover Analysis
PSDM	Probabilistic Seismic Demand Model
PSF	Period Shift Factor
RC	Reinforced Concrete
RSA	Response Spectrum Analysis
RSD	Response Spectrum Displacement

SDOF	Single Degree OF Freedom
STAAD-PRO	Structural Analysis & Aided Design Program
SW	Shear Wall
URM	Un-Reinforced Masonry

# NOTATIONS

---

## English Symbols

$C$	Capacity
$D$	Demand
$d_i$	Inter storey drift demand
$H_b$	Height of the building
$H_{eff}$	Effective height of building
$g$	Acceleration due to gravity
$k$	Lateral stiffness of structure
$m_x$	Mean
$P_f$	Fragility function
$P[LS_i]$	Limit state probability
PGA	Peak ground acceleration
RSD	Response spectrum displacement
$S_a$	Spectral acceleration
$S_d$	Spectral displacement
$S_D$	Chosen demand
$S_C$	Chosen limit state capacity
$T_0$	Initial fundamental vibration period
$T_e$	Secant first mode vibration period

$X$	Normally distributed variable
Greek Symbols	
$\theta$	Inter storey drift angle
$\theta_{\max}$	Maximum seismic drift angle
$\theta_{\text{avg}}$	Average drift angle
$\beta$	Periodic shift factor
$\lambda$	Drift factor
$\Delta_{\text{roof}}$	Lateral displacement at roof level
$\sigma_x$	Standard deviation
$\phi$	Cumulative distribution function
$\beta_c$	Dispersions in capacities
$\beta_{\text{d/IM}}$	Dispersions in the intensity measure
$\beta_M$	Dispersions in modelling
$\beta_q$	Quality and completeness of the nonlinear analysis model

# Chapter 1

## INTRODUCTION

---

### 1.1 MASONRY INFILLED FRAMES

The construction of multi-storey masonry infill (MI) reinforced concrete (RC) buildings has been practice in India for the last few decades. However, the quality of design and construction remains variable in all over India. Indeed, even in earthquake-prone regions of India, basic configuration taking into account gravity burden keeps on being honed without considering the lateral load following up on to the structure and the seismic vulnerability of the RC structure. Out of all the urban development in India may be just 10% of all development comprises of reinforced cement (RC) structures of which those satisfy with seismic prerequisites are immaterial in number. A large portion of this development in India has been outlined just for gravity loads, infringing upon the Code of Indian Standards for earthquake-resistant design IS 1893. These structures performed inadequately and have encountered a few harm amid the 2001 Bhuj seismic earthquake (Fig. 1.1).



**Fig. 1.1:** Damage of MI RC building amid 2001 Bhuj Earthquake ([www.nicee.org](http://www.nicee.org))

Masonry infill walls restricted by RC outlines in all the sides assume a vital part in opposing the lateral seismic loads on structures. infille walls have a high lateral stiffness and low deformability (Moghaddam and Dowling, 1987). Therefore presentation of masonry infilled walls in reinforced cement (RC) casings changes the lateral-load transfer mechanism of the structure from transcendent frame action to dominating truss action (Murty and Jain, 2000), as demonstrated in Fig. 1.2, which decreases the bending moments of the structure and increases axial forces acting up on to the individual members.

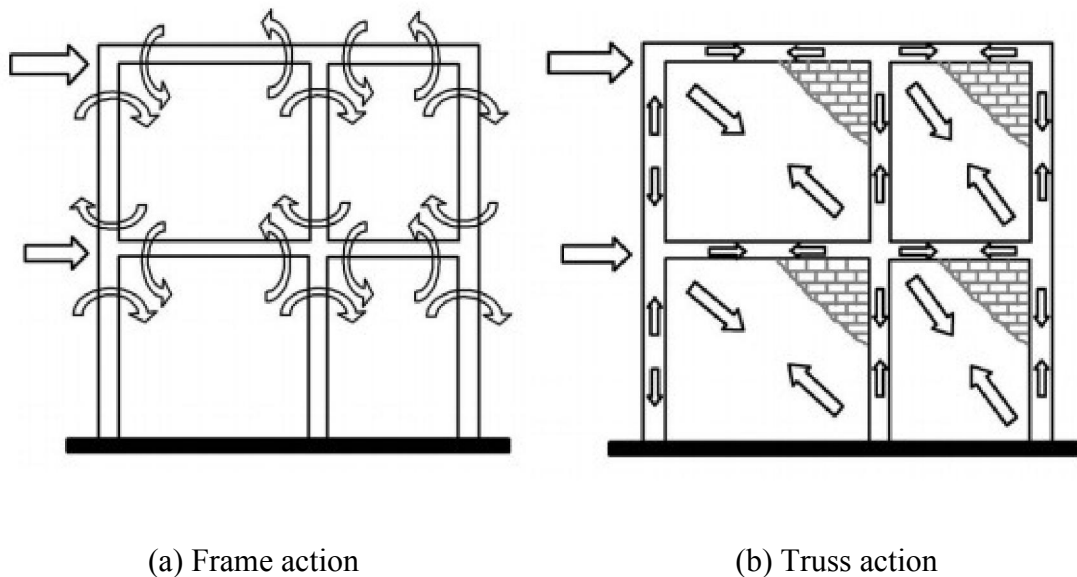


**Fig. 1.2:** Change of lateral-load transfer mechanism due to infill walls (Ref. Murty and Jain, 2000).

## 1.2 FRAGILITY CURVES

Fragility curves are graphically characterize the seismic risk and the degree of damage on to the structure under the impact of strong ground motion of different intensity. In fragility analysis the damage likelihood of RC structures are the capacity of intensity measures (IMs), for example, peak ground acceleration (PGA), spectral acceleration ( $S_a$ ) and spectral displacement ( $S_d$ ). In the past studies, fragility curves for masonry infilled reinforced concrete structures are gotten by both linear and non-linear analytical methods like non-linear time history analysis (NTHA), incremental dynamics analysis (IDA) and pushover analysis (POA). In this study, an explanatory methodology i.e. coefficient based method (Lee and Su, 2012) and SAC FEMA technique (Cornell *et al.*, 2002) was embraced to build up the fragility curves for masonry infilled RC structures.

## 1.3 BACKGROUND AND MOTIVATION

With the progression of computational advances, the demands (or limits) of structures and intensity measures (IMs) can be resolved through non-linear time history analysis (NTHA), pushover analysis (POA) (ATC, 1996; Fajfar and Gašperšič, 1996; Chopra and Goel, 1999; Fajfar, 2000; Chopra and Goel, 2002; Kalkan and Kunnath, 2007) and incremental dynamics analysis (IDA) (Vamvatsikos and Cornell, 2002; Han and Chopra, 2006), which are liable to create the best estimation of a structures seismic parameters. Then again, a detailed and time-consuming well-calibrated analytical finite element method alongside nonlinear material properties of every auxiliary segment ought to require for leading the nonlinear seismic fragility analysis.

The coefficient-based technique (Lee and Su, 2012) does not oblige a dreary or prolonged finite element analysis; rather, it is a simplified methodology for evaluating the spectral acceleration and displacement of structures subjected to tremors. These coefficient-based methods concentrate in determining the seismic capacity or demand of structures in terms of the inter-story drift ratio by multiplying drift factors ( $\lambda$ ). The precision of these coefficient-based seismic evaluation systems depends emphatically on the proposed drift-related factors, which are regularly decided and aligned through numerical simulation results acquired from the nonlinear time history analyses of structures subjected to different earthquake motions.

SAC FEMA technique (Cornell *et al.*, 2002) added to a probabilistic structure for seismic configuration and evaluation of RC structures in terms of seismic demand and capacity tending to the vulnerabilities in in hazard, structural, damage, and loss investigations. Structural-demand versus seismic-intensity connections was resolved from non-linear time history investigation. The structural demand was surveyed utilizing a suite of ground movements and the median structural demand was represented by a log linear function.

## 1.4 RESEARCH OBJECTIVES

The present study is focused on the comparison of fragility curves two established methods for RC frames.

- Validate and Develop fragility curves of Typical RC frames with number of stories ranging from two to six stories using coefficient based method (Method I) proposed by Lee and Su (2012)
- Development of seismic fragility curves for the same frames based on SAC FEMA method (Cornell *et al.*, 2002) (Method II).



- A critical comparison of the fragility curves between two methods (Method I and II)

## **1.5 SCOPE OF THE STUDY**

- The present study is limited up to six-storey masonry infilled RC frame structures.
- The masonry infilled RC structures consider in design are regular in plan and uniform elevation.
- The plan asymmetry arising from infill walls or the out-of-plane action of infill walls are not considered in this study.

## **1.6 METHODOLOGY**

In order to achieve the objectives the step by step procedure is worked out as given below.

- Validation study of coefficient based method for different seismic performance level using published results obtained from shaking table test.
- Design of two, four and six storey masonry infilled reinforced concrete building and assigning its geometry and material property.
- Estimation the coefficient based parameters i.e. inter storey drift ratio (IDR) and period shift factor (PSF) and drift factor ( $\lambda$ ) of the designed structure using coefficient based method for synthetic ground motions.
- Determination spectral acceleration and spectral displacement of the RC building for various performance levels.
- Development of seismic fragility curves for two, four and six storey masonry infilled reinforced concrete building for various performance level are obtained using coefficient based method.

- Comparison of the fragility curves obtained from coefficient based method with SAC FEMA method at the damage state (CP state) performance level.

## **1.7 ORGANIZATION OF THESIS**

(Chapter 1): A brief presentation of masonry infilled (MI) reinforced cement (RC) structures, alongside the brief portrayal of fragility curve of masonry infilled reinforced concrete building are discussed about in this starting section. The objectives and scope of the present exploration work alongside the methodology are likewise examined here.

(Chapter 2): This chapter discuss about the literature review on different topics related to masonry infilled (MI) reinforced concrete (RC) buildings. An overview of the performance characteristic and different prescribed damage state is also presented here. Further, the detail methodology and the seismic fragility analysis procedure of both coefficient based method and SAC FEMA technique for seismic risk assessment are discussed and finally the validation study of coefficient based method are completed toward the end of this article.

(Chapter 3): This part inspects about the advancement of the fragility curves for different performance levels utilizing coefficient based technique furthermore section shows the examination of fragility curves created utilizing coefficient based system and SAC-FEMA technique for diverse storey frames.

(Chapter 4): The last section shows the synopsis and critical conclusions drawn from the present study. This part additionally examines the degree for future study in the range of masonry infilled reinforced cement structures.

### LITERATURE REVIEW & VALIDATION

---

#### 2.1 INTRODUCTION

In this study, the advancement of fragility characteristics masonry infilled (MI) Reinforced Concrete (RC) structures are exhibited. Fragility examination is to gauge the seismic vulnerability of structures under the impact of ground movement. Fragility curves (or characteristics) are critical for evaluating the general seismic damage to the structures and to foresee the monetary misfortune assessment, debacle reaction arranging, retrofitting of structures for a past quake occasions. Fragility curves, which graphically speak to the seismic risk to a structure, which characterizes the probabilities of surpassing distinctive recommended damage levels as a component of the intensity measures ( $IMs$ ) and the peak ground acceleration (PGA), spectral acceleration ( $S_a$ ) or spectral displacement ( $S_d$ ) of a tremor. The fragility analyses (Casciati and Faravelli, 1991; Mosalam *et al.*, 1997; Cornell *et al.*, 2002; Lang and Bachmann, 2004; Akkar *et al.*, 2005; Kircil and Polat, 2006; Ramamoorthy *et al.*, 2006; Ellingwood *et al.*, 2007; Lagaros, 2008; Seyed *et al.*, 2010; Howary and Mehanny, 2011), for assessing the seismic dangers of structures has been generally examined.

In the fragility investigation, the demands (or limit) of the structures are lognormally distributed (Cornell *et al.*, 2002) i.e. the relationship between the demand and IMs can be ordinarily anticipated by a two-parameter model (Cornell *et al.*, 2002; Choi *et al.*, 2004; Ramamoorthy *et al.*, 2006; Ellingwood *et al.*, 2007; Konstantinidis and Makris, 2009). In view of the lognormal distribution, the scatter plots of the demands of structures and comparing IMs are articulated on a

logarithmic scale; consequently, a regression analysis can be performed to acquire the best-fitting straight regression comparison, bilinear regression equation (Ramamoorthy *et al.*, 2006), or quadratic relapse mathematical statement (Pan *et al.*, 2010) from the power model. The logarithmic middle and standard deviation of the information concerning the relapse comparisons can be acquired by a basic factual examination. The likelihood of surpassing distinctive damage states for a predetermined IM can be resolved once the logarithmic mean and standard deviation are discovered utilizing the standard ordinary dispersion capacity (Casciati and Faravelli, 1991). The damage conditions of structures are immediate occupancy (*IO*) state, life safety (*LS*) state, and collapse prevention action (*CP*) are indicated by different IDR levels for the execution based configuration proposed by outline rules (ATC, 1996; ASCE, 2000).

## **2.2 DEFINITIONS**

In this article a brief review is of the Intensity Measures, the building performance level or (Damage States), the Damage Measures and the methods that has been used for the fragility analysis has described.

### **2.2.1 Intensity measures**

An Intensity Measures (IMs) is the ground motion parameter against which the probability of exceedance of a given damage state is plotted. There are two main classes of IMs: the empirical and the instrumental. The empirical IMs, different macroseismic intensity scales are derived for qualitative assessments of the damage. Such intensity scales are: the Mercalli-Cancani-Sieberg Intensity Scale (MCS), the Modified Mercalli Intensity Scale (MMI), the European Macroseismic Scale (EMS-98) etc. Macroseismic intensity scales have a wide range of applications in the field of fragility analyses. The instrumental IMs, the severity of the

ground shaking can be recorded by accelerograms. The preferred IMs that are used for seismic vulnerability assessment of buildings are:

- a) Peak ground acceleration,  $PGA$
- b) Peak ground velocity,  $PGV$
- c) Spectral acceleration,  $S_a$
- d) Spectral displacement,  $S_d$

### **2.2.2 Building performance levels**

These execution attributes of a building will be specifically identified with the degree of damage maintained by the building amid a seismic tremor. The Structural Performance of a building should be chosen from four Structural Performance Levels Ranges characterized in this segment (ASCE, 2000). The Structural Performance Levels of a building are Immediate Occupancy, Life Safety, Limited Safety Range and Collapse Prevention. The four Structural Performance Levels characterized in this standard have been chosen to correspond with the most usually determined basic execution necessities. The Structural Performance Ranges helps clients to redo their building Rehabilitation Objectives.

#### **(a) Immediate Occupancy (IO) Structural Performance Level**

Structural Performance Level, Immediate Occupancy, should be characterized as the post-quake damage state in which just extremely restricted auxiliary damage has been happened and that remaining parts safe to involve, basically holds the configuration quality and firmness of the structure. The basic damage is low, and albeit some minor auxiliary repairs may be suitable, these would for the most part not be needed before re inhabitation.

### **(b) Life Safety (LS) Structural Performance Level**

Structural Performance Level, Life Safety, should be characterized as the post-tremor damage state in which critical harm to the structure has happened, yet some edge against either incomplete or complete auxiliary breakdown remains. Some basic components and parts are extremely harmed, however this has not brought about huge perils, either inside or outside the building. Damages may happen amid the seismic tremor; then again, the general danger of life-undermining harm as an aftereffect of basic damage is relied upon to be low. It ought to be conceivable to repair the structure or introduce interim propping before reoccupancy.

### **(c) Limited Safety Structural Performance Range**

Structural Performance Range, Limited Safety should be characterized as the ceaseless scope of damage states between the Life Safety Structural Performance Level and the Collapse Prevention Structural Performance Level.

### **(d) Collapse Prevention (CP) Structural Performance Level**

Structural Performance Level, Collapse Prevention, might be characterized as the post-tremor damage state in which the building is very nearly halfway or aggregate breakdown. Considerable harm to the structure has happened, including significant degradation in the stiffness and strength of the lateral-force resisting system and also large permanent lateral deformation in vertical-load-carrying capacity. The structure may not be actually technically practical to repair and is not alright for reoccupancy.

## **2.2.3 Seismic fragility function methods**

In the estimation of the fragility capacities there is an awesome level of instability included in every progression of the technique. This vulnerability is because of the variability in the ground

motion qualities, the analytical modelling, the materials utilized and the meaning of the damaged states. The different routines for the seismic vulnerability has been grouped into four categories: empirical, expert opinion based, analytical and hybrid.

#### **(a) Empirical methods**

Experimental fragility curves (Calvi *et al.*, 2006) are built utilizing insights of the watched damage from past seismic tremor occasions, , for example, information gathered by post-quake overviews. This technique utilizes the observational information in the most practical route to model fragility curves however it is hard to deliver the fragility curve because of the inadequacy and inadequacies in the study and the blunders created in the reckoning of the seismic information and the post-preparing. The main types of empirical methods are:

- a) The Damage Probability Matrices (DPM)
- b) The Vulnerability Index Method
- c) The Continuous Vulnerability Functions

#### **(b) Expert opinion-based methods**

Expert opinion-based fragility curves depends on the judgment and the information of the experts. These experts are asked to give the detail estimation of the probability of damage for different types of structures and several levels of ground shaking from the past earthquake events. This method is not affected by the limitations regarding the quantity and quality of structural damage. However, the results are strictly correlated with the individual experience of the experts for the better estimation of fragility curve.

### **(c) Analytical methods**

Analytical methods describe the step by step algorithms for detailed study of seismic vulnerability of the structures and to estimate various characteristics of building stock and hazard. Analytical fragility curves are constructed for prescribed damage states and are simulated from analyses of structural models under increasing earthquake intensity. The application of the analytical methods might be limited by the computational effort of the analyses. To reduce the computational effort, simplified analytical models are often used, with large number of analyses, such that the uncertainties can be adequately predicted.

Seismic vulnerability can be evaluated using one of the following methods:

- a) Lateral force analysis (linear)
- b) Modal response spectrum analysis (linear)
- c) Non-linear time history dynamic analysis (NTHA)
- d) Non-linear static (pushover) analysis (POA)
- e) q-factor approach

Especially in the last few decades many studies focused on the seismic fragility functions for RC structures were based on analytical methods.(Dumova-Jovanoska, 2000; Erberik and Elnashai, 2004; Akkar *et al.*, 2005; Kircil and Polat, 2006; Oropeza *et. al.*, 2010) are some literature studies based on analytical methods.

### **(d) Hybrid methods**

Hybrid fragility curves are based on the combination of different methods for damage prediction and loss evaluation. This method aim is to compensate the lack of observational data,



the deficiencies of the structural models and the subjectivity in expert opinion data. (Barbat *et al.*, 1996; Kappos *et al.*, 2006) are some literature studies based on hybrid methods.

## **2.3 REVIEW OF PREVIOUS STUDIES BY ANALYTICAL METHOD**

Lee and Su (2012) studies the seismic fragility investigation of masonry infilled (MI) reinforced concrete (RC) structures utilizing a coefficient-based system. The coefficient-based system is an improved technique without finite element analysis for assessing the spectral acceleration and displacement of buildings subjected to earthquakes. The coefficient based parameters, for example, inter-storey drift ratio (IDR) and period shift factor (PSF) are obtained from the shaking table tests. A regression analysis was performed to acquire the best-fitting mathematical statements for the inter-storey drift ratio (IDR) and period shift factor of masonry infilled (MI) reinforced concrete (RC) structures because of the peak ground acceleration. The spectral acceleration and spectral displacement demand is obtained from seismic coefficient. Spectral acceleration- and spectral displacement-based fragility curves for different damaged states were then built utilizing the coefficient-based strategy.

Mosalam *et al.* (1997) delivered vulnerability curves for low-ascent masonry infilled RC structures for gravity loads. Pushover analyses were performed, to focus the properties of cement, steel and masonry properties, in request to acquire trilinear capacity curves. The fragility investigation were accepted to take after a lognormal conveyance with expected coefficients of variety. Nonlinear examination is done of 800 fake accelerograms information for a SDOF structure. The Monte Carlo procedure was performed to create 200 capacity curves for each accelerogram. Relationship was found with fragility curves acquired from the ATC-13 damage probability frameworks.

Cornell *et al.* (2002) built up a probabilistic system for seismic outline and appraisal of structures in a demand and capacity format tending to the vulnerabilities in hazard, structural, damage, and loss analyses. Demand and capacity were expressed in terms of the maximum inter-story drift ratio with a nonlinear dynamic relationship using ground motions. The median with logarithmic standard deviation obtained from lognormally distributed function. The SAC FEMA method used to provide the framework for probabilistic recommendations of design guidelines.

Ellingwood (2001) studies the seismic fragilities examination of regular low-to-mid-ascent steel and reinforced concrete structures and its plan and development works on utilizing SAC FEMA technique. This paper delineated a straightforward strategy for the probabilistic investigation of building reaction to comprehend the building conduct. Uncertainty in response of structures to seismic tremor ground movement is because of the peak ground motion intensity, time-varying amplitude and strong motion duration and frequency content, and design and construction practices. Fragility curve depicts the probability of exceedance of damage and are vital for annihilation and loss expectation and hazard response projection. Additionally, an examination investigation of these fragilities curves consolidated in HAZUS conveys suggestions for damage and loss estimation.

Goulet *et al.* (2007) Seismic execution evaluation of RC moment resisting-frame composed per current (2003) construction law procurements. The nonlinear dynamic structural simulations utilized for the damage investigations, and misfortune estimation. The chose ground movement records for nonlinear dynamic analyses that are communicated as far as a response spectral value at the building's fundamental period. It is critical to consider the response spectral shapes, particularly when considering higher risk levels. The nonlinear dynamic simulation results are

utilized for computing the methods and coefficients of variety. The fragility functions used to express the probabilities of segment damage.

Özer and Erberik (2008) Produced vulnerability curves for RC frames in Turkey. 3, 5-, 7 and 9-story RC outlines with poor, medium and great seismic outlined rules with shifting Concrete and steel quality and modulus of flexibility. Four damage states were presents as slight or no damage , huge damage , extreme damage and breakdown or collapse . The seismic interest were acquired regarding most extreme between inter-storey drift ratio for distinctive arrangements of ground movement records by performing non-linear time-history analyses. Fragility curves are, plotted versus PGV that were produced in this study.

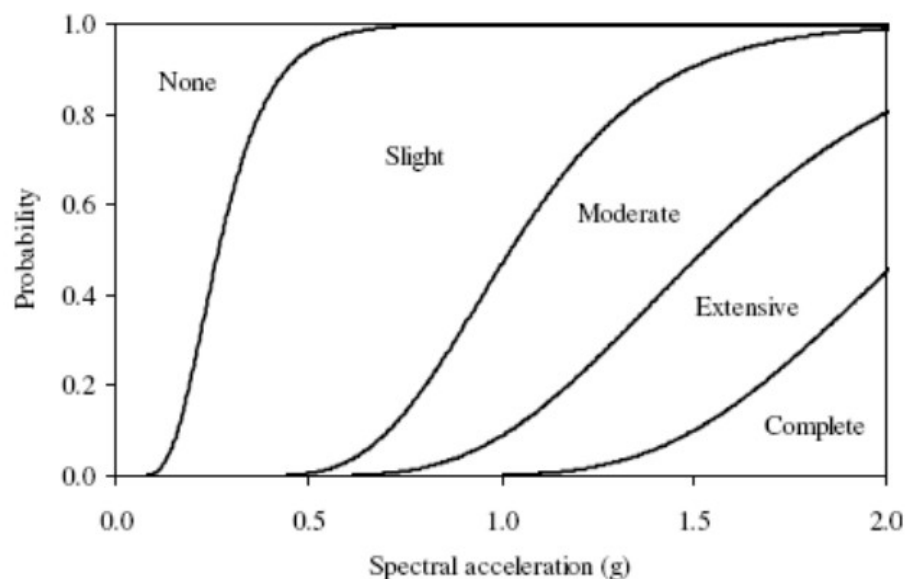


**Fig. 2.1** Spectral acceleration-based fragility curves. (Ref. - Özer & Erberik, 2008)

Akkar *et al.* (2005) created vulnerability curves for low-ascent and mid-ascent infilled RC outline structures. Pushover analyses of 32 current structures were performed to characterize the base shear limit, period and extreme story drift of the structures with low-level of seismic outline. Nonlinear dynamic analyses were then performed for 82 recorded accelerograms. The

quantity of stories was found to have a noteworthy impact on the likelihood of surpassing the moderate and the extreme severe damage limit states (LS). Spectral displacement ( $S_d$ ) corresponded preferable with PGV over PGA up, for larger amounts of damage.

Kappos *et al.* (2006) presents vulnerability curves for RC frame structures, and for unreinforced masonry (URM) structures, as per a hybrid method. This strategy consolidates measurable information as far as PGAs and/or spectral displacements which got from non-linear dynamic or static analyses. Vulnerability curves were determined regarding PGA, and spectral displacement ( $S_d$ ). Investigations of a few distinctive Low-ascent, mid-ascent and high-ascent Reinforced Concrete (RC) structures were considered; everyone was accepted to have three diverse setups (bare, regularly infilled and soft delicate ground story building). Four classes of seismic outline were considered: no code, low code, moderate code and high code. Inelastic static and dynamic time-history investigations were done.

Zhu and Su (2007) studies the forecast of the seismic drift demand and capacity of existing structures and foresee the potential seismic risks and auxiliary, damage. The thorough synopsis of configuration and specifying routine of concrete structures, trailed by seismic outline parameter drift ratio, ductility capacity, stiffness variation and non-linear damping properties and the non-seismically outlined of reinforced concrete parameters were acquired. An immediate displacement based system utilized for the forecast of the most extreme drift demands, period shifting, stiffness degradation, non-linear damping of the current building model.

## 2.4 METHODOLOGY

### 2.4.1 Coefficient-based method (Lee and Su, 2012)

The coefficient based strategy is a simplified method that does not oblige much concentrated finite element analysis to survey the spectral acceleration and displacement of building subjected to a quake ground movement. Coefficient-based techniques for deciding the seismic inter-story drift demand and limit of structures have been considered broadly (Miranda, 1999; Gupta and Krawinkler, 2000; Zhu *et al.*, 2007; Tsang *et al.*, 2009; Lee and Su, 2012; Su *et al.*, 2012). The precision of these coefficient-based seismic appraisal systems depends firmly on the proposed drift related factors, which are regularly decided and aligned through numerical simulation results acquired from the nonlinear time history investigations of structures subjected to different tremor movements.

In fragility analyses, the demand ( $D$ ) of a structure is log normally distributed (Cornell *et al.*, 2002; Konstantinidis and Makris, 2009), i.e. log normally distribute variable  $D$  is identified with an ordinarily appropriated variable  $X$  by  $\ln(D)$ . The demand and capacity of a structure can be estimated by a generalized form by a power model as follows:

$$D = a (IM)^b \quad (2.1)$$

Where  $IM$  stands for intensity measure,  $a$  and  $b$  are regression coefficients. The regression coefficients can be represented in logarithmic form as:

$$X = \ln(D) = \ln(a) + \ln(IM) \quad (2.2)$$

The mean of  $X$  can be, estimated as (Konstantinidis and Makris, 2009):

$$m_x(IM) = \ln(a IM^b) \quad (2.3)$$

The standard derivation of  $X$  can be estimated as:

$$\sigma_X = \sigma_{\ln D} = \sqrt{\frac{1}{n-2} \sum_{i=1}^n \left[ \ln \left( \frac{\delta_i}{a IM_i^b} \right)^2 \right]} \quad (2.4)$$

Where  $\delta_i$  is the demand value for  $n$  number of records.

For the lognormally distributed arbitrary variable  $D$ , the fragility function ( $P_f$ ), which gives the likelihood of exceedance of demand  $D$  for a threshold capacity or drift capacity,  $C$ , for a contingent ground movement intensity measure ( $IM$ ), can be obtained as follows:

$$P_f \equiv P(D > C | IM) = 1 - \phi \left( \frac{\ln C - m_x(IM)}{\sigma_X} \right) \quad (2.5a)$$

$$= 1 - \Phi \left( \frac{1}{\sigma} \ln \frac{C}{a IM^b} \right) \quad (2.5b)$$

$$\phi \left( \frac{\ln C - m_X(IM)}{\sigma_X} \right) = \int_{-\infty}^u \frac{1}{\sqrt{2\pi\sigma_X}} \exp \left( -\frac{u^2}{2} \right) du \quad (2.6)$$

$$u = (\ln C - m_X(IM)) / \sigma_X \quad (2.7)$$

Where  $\phi$  is the cumulative distribution function of a standard normal variable which has a mean of zero and standard variation of unity.

Once the mean ( $m_x$ ) (varying with  $IM$ ) and standard deviation ( $\sigma_x$ ) are obtained from Eq 2.3 and 2.4. The fragility curves can be constructed for various damage states or capacities. The parameter,  $IDR(\theta)$  is considered as demand and parameter  $S_a$  (or  $S_d$ ) is considered as  $IM$ .

The spectral displacement ( $S_d$ ) of the masonry infilled (MI) Reinforced Concrete (RC) building at any loading state can be represented in Eq. 2.8 according to the building model illustrated in Fig. 2.2 (Zhu *et al.*, 2007; Su *et al.*, 2008; Tsang *et al.*, 2009; Su *et al.*, 2011; Lee and Su, 2012; Su *et al.*, 2012):

Spectral displacement demand ( $S_d$ ),

$$S_d = \frac{H_b \theta}{\lambda} \quad (2.8)$$

Where,

$\lambda$  is the drift factor

$H_b$  is the height of the building

$\theta$  is the maximum IDR for the corresponding PGA

Spectral acceleration demand ( $S_a$ ) can be related to  $S_d$  as,

$$S_a = S_d \left( \frac{2\pi}{T_e} \right)^2 \quad (2.9a)$$

$$= \frac{H_b}{T_0^2} \frac{(2\pi)^2}{\lambda} \frac{\theta}{\beta^2} \quad (2.9b)$$

Where,

$T_0$  is the initial fundamental vibration period of the undamaged structure

$\beta$  is the periodic shift factor (PSF)

Equivalent fundamental (first mode) vibration period due to stiffness deterioration,

$$T_e = \beta T_0$$

The Eq. 2.8 and 2.9 are used to estimate the spectral displacement and spectral acceleration demands of masonry infilled (MI) Reinforced Concrete (RC) structures for any IDR demand. Moreover, the spectral displacement and acceleration demands obtained from Eqs. (2.8) and (2.9) for a specific IDR ( $\theta$ ) may be regarded as the spectral displacement and acceleration capacities of the structure if the IDR reaches a certain damage state (or performance level).

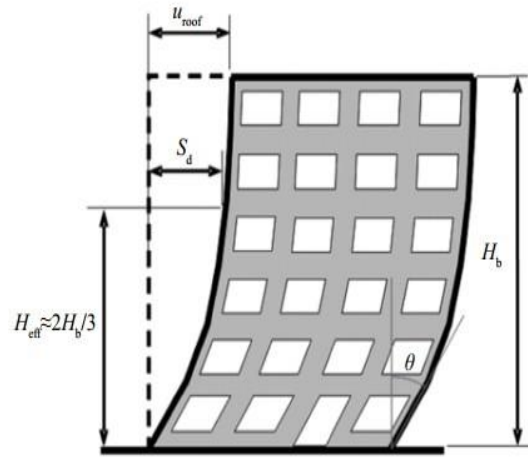


**Fig. 2.2** Deformation model of a masonry in-filled reinforced concrete building (Ref. Su *et al.*, 2012).

#### 2.4.1.1 Periodic shift factor ( $\beta$ )

Under the strong ground movement, masonry infilled RC structures experience inelastic deformations because of, which breaking and sliding block masonry. The decrease in firmness prompts protracting of the basic structural period under seismic activities. The period shift factor ( $\beta$ ) can be obtained from Eq. 2.10 for the impact of period lengthening (stiffness degradation factors)

$$PSF(\beta) = \frac{T_e}{T_0} \quad (2.10)$$



### 2.4.1.2 Definition of drift factors for building

A disentangled hypothetical system for demonstrating the greatest seismic inter-story drift angle  $\theta_{max}$  of multi-story structures has been created by (Chandler *et al.* 2002a, 2002b) and later in (Sheik, 2005), demonstrated in fig. 2.3

The maximum seismic drift angle  $\theta_{max}$  for the joined vibration modes can be written:

$$\theta_{max} = \lambda_1 \lambda_2 \lambda_{avg} \frac{RSD_1}{H_b} \quad (2.11)$$

Where,

$RSD$  is the seismic response spectral displacement at the fundamental mode period.

$H_b$  is the height of the building.

$\lambda_1, \lambda_2, \lambda_{avg}$  are the dynamic drift coefficients.

$\Delta_{Iroof}$  is the lateral displacement at roof level (due to the fundamental vibration mode only).

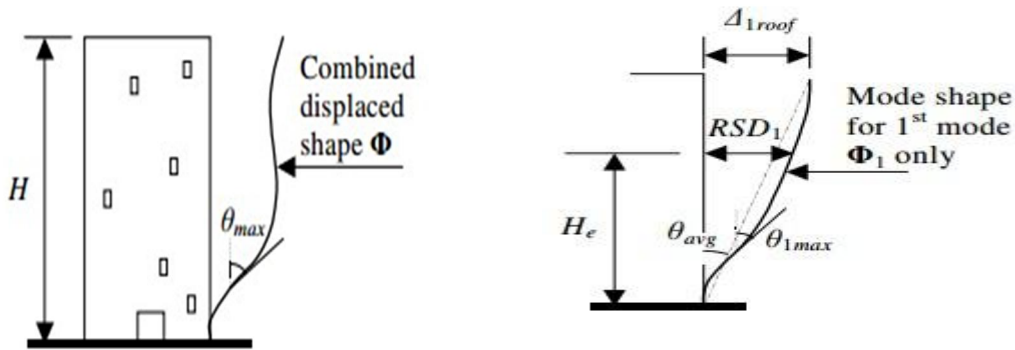


**Fig. 2.3** Illustration of drift angle  $\theta_{max}$ ,  $\theta_{1max}$  and  $\theta_{avg}$  (Ref. Sheikh, 2005).

To start with, the average seismic inter-story drift angle  $\theta_{avg}$  can be characterized as (considering the fundamental mode only):

$$\theta_{avg} = \frac{\Delta_{1roof}}{H_b} \quad (2.12)$$

$\Delta_{1roof}$  the lateral displacement at roof level can be associated with the seismic response spectral displacement  $RSD_1$  at the fundamental mode by the multiplier  $\lambda_{avg}$  as:

$$\lambda_{avg} = \frac{\Delta_{1roof}}{RSD_1} \quad (2.13)$$

The maximum inter-story drift angle  $\theta_{1max}$  (due to the fundamental vibration mode only) can be associated with the average drift angle by the drift multiplier  $\lambda_1$  can be evaluate from Eq. 2.14 as:

$$\lambda_1 = \frac{\theta_{1max}}{\theta_{avg}} \quad (2.14)$$

The maximum drift angle ( $\theta_{max}$ ) can be identified with  $\theta_{1max}$ , considering higher lateral modes of vibration, by the drift multiplier  $\lambda_2$  can be evaluate from Eq. 2.15 as:

$$\lambda_2 = \frac{\theta_{max}}{\theta_{1max}} \quad (2.15)$$

For the higher-mode drift multiplier  $\lambda_2$ , is depends on the seismic tremor ground movement, on the proportion of  $RSD_2/RSD_1$ .  $RSD_2$  is the seismic response spectral displacement at the second modular period, and  $\lambda_2$  can be evaluate from Eq. 2.16 as:

$$\lambda_2 = 0.35 + 2.0 \frac{RSD_2}{RSD_1} \geq 1 \quad (2.16)$$

The combined dynamic drift coefficient  $\lambda_{max}$  as:

$$\lambda_{max} = \lambda_1 \lambda_2 \lambda_{avg} \quad (2.17)$$

Thus, the maximum seismic drift angle  $\theta_{max}$  because of the combined vibration modes:

$$\theta_{max} = \lambda_{max} \frac{RSD_1}{H_b} \quad (2.18)$$

#### 2.4.2 Step wise procedure for Coefficient-based method (Lee and Su, 2012)

The step wise procedure to develop the fragility curves as per the coefficient based method is given below.

- Estimate the maximum Inter-storey drift (IDR) ratio values for different peak ground acceleration (PGA) values for the frame selected from a number of ground motions. This may be obtained from existing shake table experiment or computational methods such as nonlinear dynamic analysis of the selected frame. Minimum four pair of values of PGA and IDR drift is required. Fit a logarithmic relationship for PGA values in terms of IDR,  $PGA = f(IDR)$ .
- Period shift factor ( $\beta$ ) using Eq.2.10. The fundamental time period ( $T_0$ ) and time period of the damaged building ( $T_e$ ) can be obtained either from shake table test or computationally. For each PGA values the corresponding period shift factors are computed. Fit a logarithmic linear expression for period shift factor ( $\beta$ ) in terms of PGA as  $\beta = f(PGA)$ .

- Compute drift factor ( $\lambda$ ) for the masonry infilled RC building using Eq. 2.17 from the maximum, average inter-storey drift ratio for first mode shape and maximum inter-storey drift ratio from combined mode shape.
- Generate PGA values for IDR values varying from 0.1% to 6% in a uniform interval. Compute period shift factor ( $\beta$ ) values for each PGA values. Compute spectral acceleration ( $S_a$ ) values for each set of values of IDR, PSF ( $\beta$ ) and drift factor ( $\lambda$ ). Estimate the spectral acceleration and spectral displacement demand for the frame using Eq. 2.8 and 2.9. Compute the mean ( $m_x$ ) and standard deviation ( $\sigma_x$ )
- Construct fragility curve using Eq. 2.5a, where  $P_f$  is the exceedance probability of IDR.

#### 2.4.3 SAC FEMA method (Cornell *et. al.*, 2002)

The fragility capacity speaks to the probability of exceedance of a chose Engineering Demand Parameter (EDP) for a chose basic structural limit state (LS) for a particular ground movement intensity measure (IM). Fragility curves are cumulative probability distributions that show the likelihood that a framework will be damaged to a given damage state or a more serious one, as a component of a specific demand. The seismic fragility,  $P_f(x)$  can be communicated in structure utilizing the accompanying mathematical statement,

$$P_f(D \geq C|IM) = 1 - \phi \left( \frac{\ln \frac{S_C}{S_D}}{\sqrt{\beta_{D|IM}^2 + \beta_C^2 + \beta_M^2}} \right) \quad (2.19)$$

where,  $D$  is the drift demand,  $C$  is the drift capacity at picked limit state,  $S_C$  and  $S_D$  are the picked limit state and the median of the demand (LS) separately.  $\beta_{d/IM}$ ,  $\beta_c$  and  $\beta_M$  are

dispersions in the intensity measure, capacities and modelling individually. A fragility curve can be acquired for distinctive point of confinement limit states utilizing Eq. 2.19

### Probabilistic Seismic Demand Model (PSDM)

The seismic interest ( $S_D$ ) is generally portrayed through probabilistic seismic demand models (PSDMs) especially for nonlinear time history analyses which will be given in terms of a suitable intensity measure (IM). It has been proposed by Cornell *et al.* (2002) (otherwise called 2000 SAC FEMA technique) for evaluation of the median demand, EDP ( $S_D$ ) can be articulated to in a summed up structure by a power demonstrate model as given in Eq. 2.20

$$EDP = a(IM)^b \quad (2.20)$$

where  $a(IM)b$  speaks to the mean inter-storey drift,  $a$  and  $b$  will be the regression coefficients of the PSDM. Eq. 2.19 can be changed for fragilities framework as:

$$P(D \geq C|IM) = 1 - \phi \left( \frac{\ln(S_C) - \ln(aIM^b)}{\sqrt{\beta_{D|IM}^2 + \beta_C^2 + \beta_M^2}} \right) \quad (2.21)$$

The dispersion,  $\beta_{D|IM}$ , of inter-storey drifts ( $d_i$ ) from the time history examination can be figured utilizing Eq. 2.22 as,

$$\beta_{D|IM} \cong \sqrt{\frac{\sum [\ln(d_i) - \ln(aIM^b)]^2}{N-2}} \quad (2.22)$$

uncertainty connected with building definition and development quality ( $\beta_c$ ) represents the likelihood that the real properties of basic structural components (e.g., material quality, segment properties, and rebar area) may be distinctive than those generally accepted to exist. For existing structures, this will depend on the quality of the accessible drawings reporting the as-constructed development, and the level of field examination performed to confirm their exactness. For new structures, this will be decided based on the actual construction with the real development outline. ATC 58(2012) suggests values for  $\beta_c$  under illustrative conditions. In the present study  $\beta_c$  is viewed as 0.25 which speaks to the building outline will be finished to a level commonplace of configuration improvement, development quality certification and assessment will be foreseen to be of constrained quality.

As indicated by ATC 58 (2012), modelling uncertainty ( $\beta_m$ ) is the outcome from mistakes in component modelling, damping and mass suppositions. With the end goal of assessing  $\beta_m$ , this uncertainty has been related with the dispersion of building definition and construction quality confirmation ( $\beta_c$ ) and the quality and fulfillment of the nonlinear analysis model ( $\beta_q$ ). The aggregate modelling dispersion can be assessed as follows:

The total modelling dispersion can be assessed as follow:

$$\beta_m = \sqrt{\beta_c^2 + \beta_q^2} \quad (2.23)$$

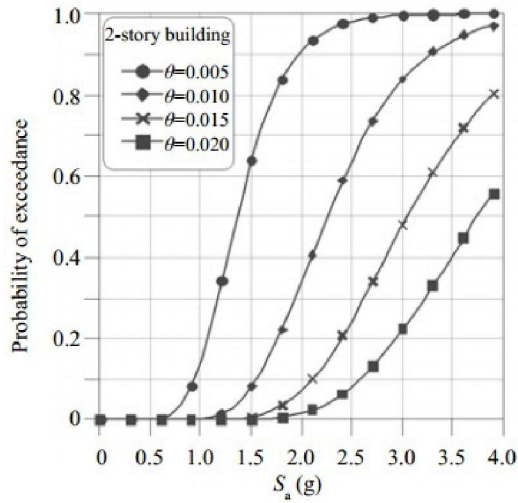
$\beta_q$  perceives that hysteretic models might not precisely capture the conduct of structural segments, regardless of the possibility that the points of interest of development are absolutely known. Estimations of  $\beta_q$  are allocated construct in light of the fulfillment of the scientific model and how well the parts deterioration and failure mechanisms are comprehended and executed. Dispersion ought to be chosen taking into account a comprehension of how delicate reaction expectations are to key structural parameters (e.g., strength, stiffness, deformation capacity, and degradation) and the degree of inelastic reaction. In this study  $\beta_q$  is assumed to be 0.25

## **2.5 VALIDATION STUDY OF THE COEFFICIENT-BASED METHOD**

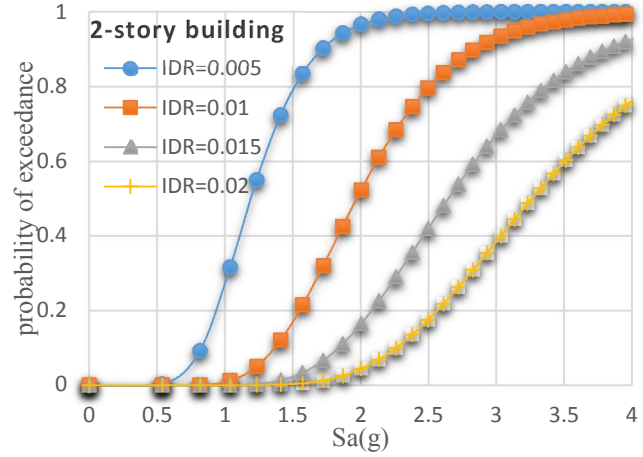
In order to validate the methodology for fragility curves, the frames considered in the study, Lee and Su (2012) is selected and the fragility curves are developed as per the step wise procedure explained in the previous section.

### **2.5.1 Validation study: Spectral acceleration ( $S_a$ ) based fragility curves**

The fragility curves developed for the two, three, four and five storey frames are shown in Figs. 2.4, 2.5, 2.6 and 2.7. It can be seen that the fragility curves on the present study is fairly matching with the published literature of Lee and Su (2012) of inter storey drift ratio of 0.5%, 1%, and 2%, which were suggested by Ramamoorthy *et al.* (2006).

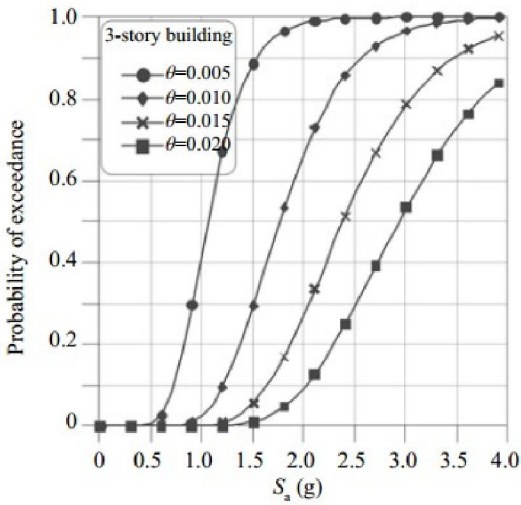


(Lee and Su, 2012)

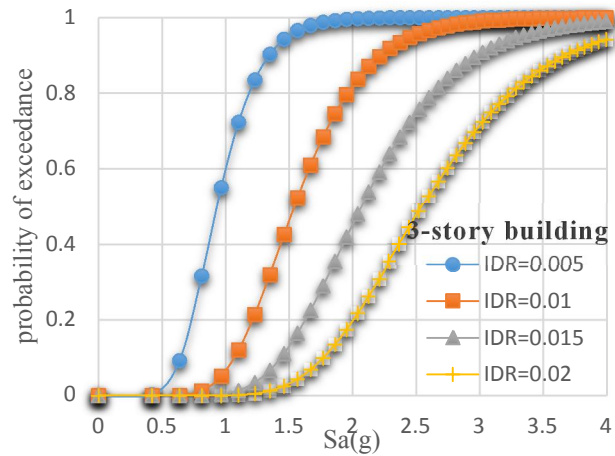


(Present study)

**Fig 2.4** Spectral acceleration ( $S_a$ ) based Fragility curves for two storey MI RC buildings



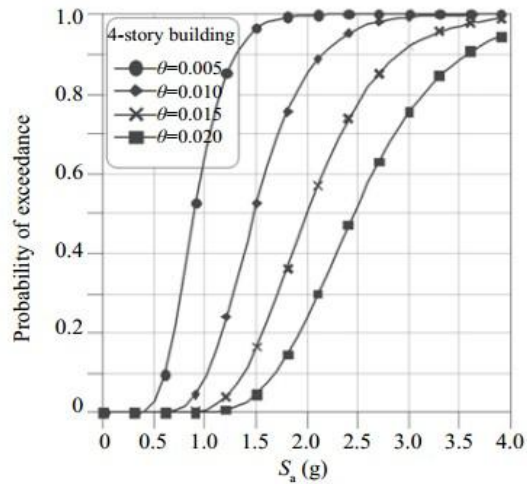
(Lee and Su, 2012)



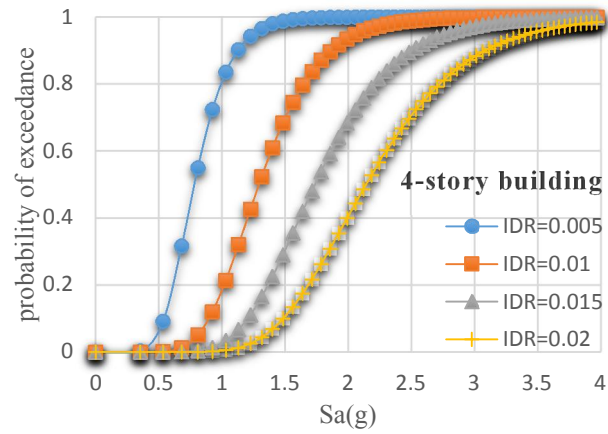
(Present study)

**Fig 2.5** Spectral acceleration ( $S_a$ ) based Fragility curves for three storey MI RC buildings



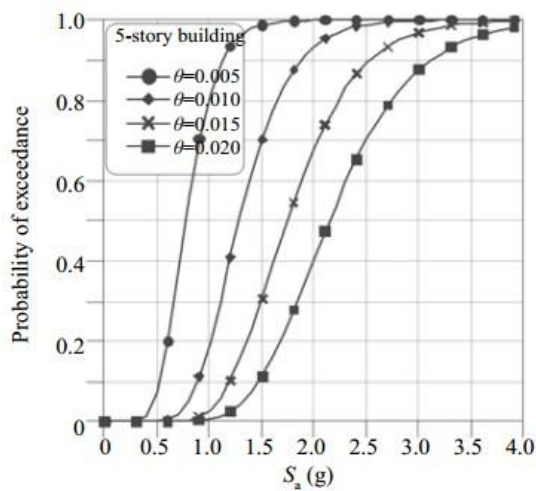


(Lee and Su, 2012)

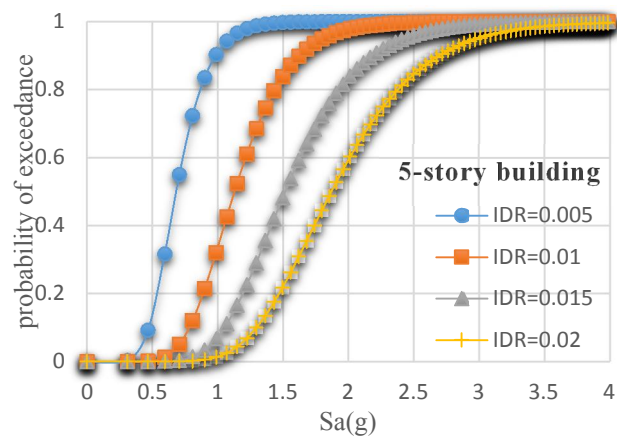


(Present study)

**Fig 2.6** Spectral acceleration ( $S_a$ ) based Fragility curves for four storey MI RC buildings



(Lee and Su, 2012)



(Present study)

**Fig 2.7** Spectral acceleration ( $S_a$ ) based Fragility curves for five storey MI RC buildings

## 2.5.2 Validation study: Spectral displacement ( $S_d$ ) based fragility curve

The spectral displacement based fragility curves developed for the two, three, four and five storey frames are shown in Figs. 2.8, 2.9, 2.10 and 2.11. It can be seen that the fragility curves on the present study is fairly matching with the published literature of Lee and Su (2012) of inter storey drift ratio of 0.5%, 1%, and 2%, which were suggested by Ramamoorthy *et al.* (2006).

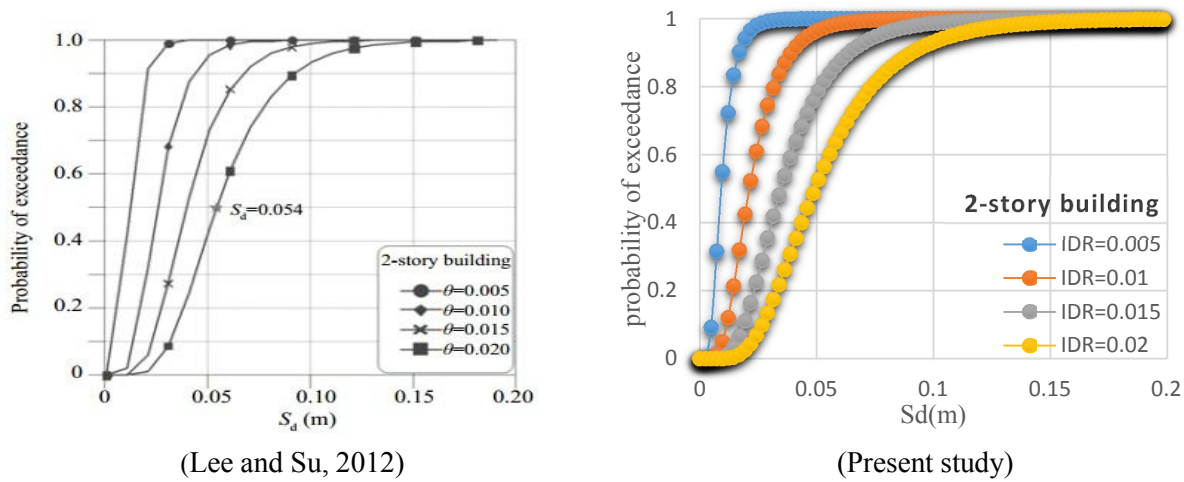


**Fig 2.8** Spectral displacement ( $S_d$ ) based Fragility curves for two storey MI RC buildings

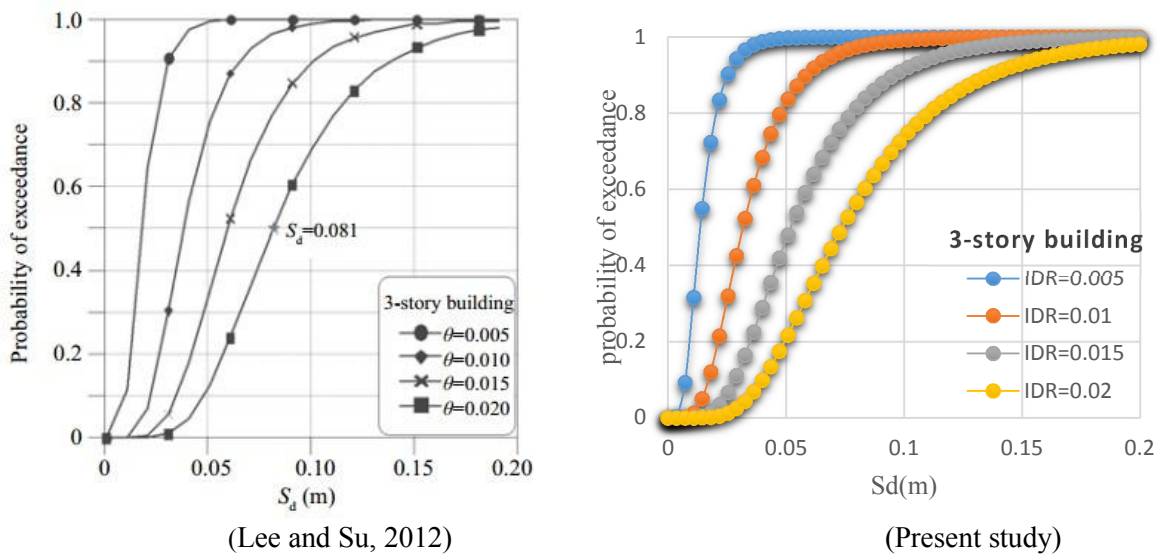
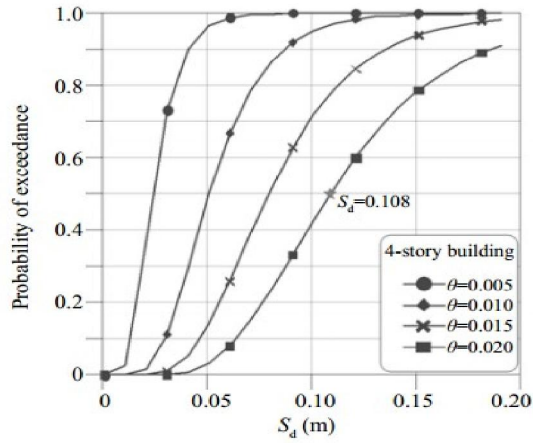
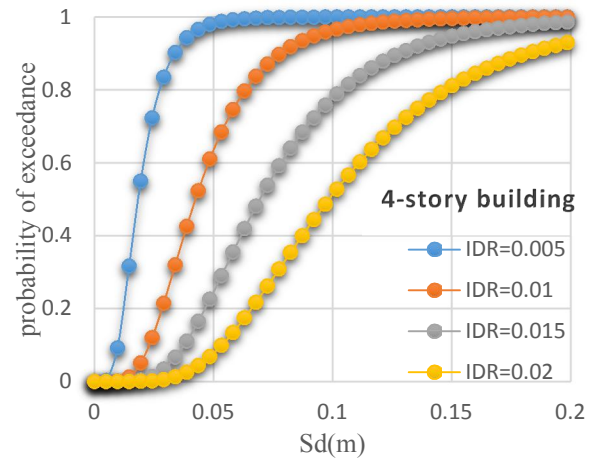


**Fig 2.9** Spectral displacement ( $S_d$ ) based Fragility curves for three storey MI RC buildings

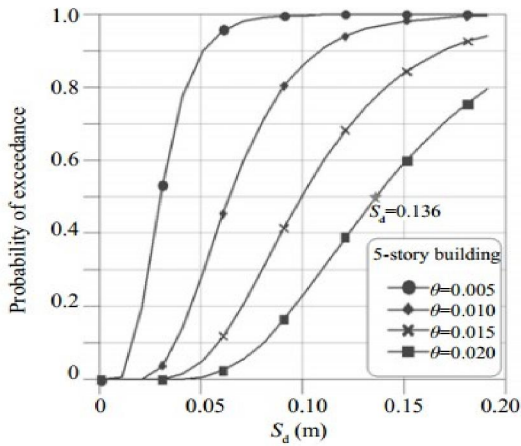


(Lee and Su, 2012)

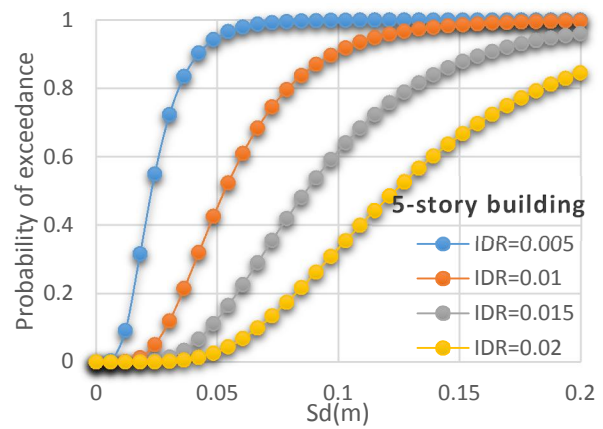


(Present study)

**Fig 2.10** Spectral displacement ( $S_d$ ) based Fragility curves for four storey MI RC buildings



(Lee and Su, 2012)



(Present study)

**Fig 2.11** Spectral displacement ( $S_d$ ) based Fragility curves for five storey MI RC buildings

## 2.6 SUMMARY

This chapter presents the detail study of the masonry infilled reinforced concrete buildings. The detail literature study on the different methods through which fragility curves can be obtained. This study depicts about the Intensity Measures, the building performance level or( the Damage States), the Damage Measures and the methods that has been used for the fragility analysis. This chapter describes the detail literature review of the fragility analysis of masonry in-filled reinforced concrete building. The fragility analysis procedure and different analytical methods to obtain the fragility curve are described in the literature review section.

The study concentrate on the seismic vulnerability assessment of masonry infilled reinforced concrete buildings and to distinguishing the damage risk of a structure influenced by ground motion of different intensity. This chapter explains the detailed step by step procedure of seismic risk assessment in a probabilistic framework using lognormal distribution. Fragility curves used to explain probabilities of exceeding different prescribed damage states (or performance levels).Finally this chapter briefly explains the coefficient based method and SAC FEMA technique used in the present study to obtain the fragility curves for the buildings. Later towards the end the validation of coefficient based method considering Lee and Su (2012) literature to design the fragility curve for different storey buildings.

### DEVELOPMENT OF FRAGILITY CURVES

---

#### 3.1 INTRODUCTION

In this chapter we discuss the development of the fragility curves by two methods such as Coefficient based method and SAC-FEMA method for masonry infilled (MI) reinforced concrete (RC) buildings having number of stories two, four and six. The Chapter starts with the description of ground motion data used for both the methods. Following the ground motion data, this chapter discuss about the development of the fragility curves using coefficient based method (Lee and Su, 2012) for various performance levels in particular Immediate Occupancy (*IO*), Life Safety (*LS*) and Collapse Prevention (*CP*). A comparison study of fragility curves developed using coefficient based method and SAC-FEMA method (Cornell et al., 2002) for different storey frames in the last part of this Chapter.

#### 3.2 METHODOLOGY

The step wise procedure to develop the fragility curves as per the coefficient based method is given below.

- Estimate the maximum Inter-storey drift (IDR) ratio values for different peak ground acceleration (PGA) values for the frame selected from a number of ground motions. This may be obtained from existing shake table experiment or computational methods such as nonlinear dynamic analysis of the selected frame. Minimum four pair of values of PGA and IDR drift is required. Fit a logarithmic relationship for PGA values in terms of IDR,  $PGA = f(IDR)$ .

- Period shift factor ( $\beta$ ) using Eq.2.10. The fundamental time period ( $T_0$ ) and time period of the damaged building ( $T_e$ ) can be obtained either from shake table test or computationally. For each PGA values the corresponding period shift factors are computed. Fit a logarithmic linear expression for  $\beta$  in terms of PGA as  $\beta = f(\text{PGA})$ .
- Compute drift factor ( $\lambda$ ) for the masonry infilled RC building using Eq. 2.17 from the maximum, average inter-storey drift ratio for first mode shape and maximum inter-storey drift ratio from combined mode shape.
- Generate PGA values for IDR values varying from 0.1% to 6% in a uniform interval. Compute PSF ( $\beta$ ) values for each PGA values. Compute spectral acceleration ( $S_a$ ) values for each set of values of IDR, PSF ( $\beta$ ) and drift factor ( $\lambda$ ). Estimate the spectral acceleration and spectral displacement demand for the frame using Eq. 2.8 and 2.9. Compute the mean ( $m_x$ ) and standard deviation ( $\sigma_x$ )
- Construct fragility curve based on coefficient based method using Eq. 2.5a, where  $P_f$  is the exceedance probability of IDR.
- Development of seismic fragility curves for the same frames based on SAC FEMA method (Cornell *et al.*, 2002) using Eq. 2.19 for the same frames.
- A critical comparison of the fragility curves between coefficient based method and SAC FEMA method

### 3.3 EARTHQUAKE GROUND MOTION DATA

Generation of fragility curves by both seismic coefficient based and SAC FEMA method require ground motion data. Thirteen pairs of ground motion data are selected from past earthquakes events in different location in India. All the selected ground motion records are available at Indian region in CESMD website (<http://strongmotioncenter.org/>). All the ground motion

earthquake records selected with PGA ranging from 0.1g to 1.48g are located with hypo-central distance 10km away from the faults. Table 3.1 presents the ground motion data used in the present study.

**Table 3.1** Selected Indian Ground motion data

S.No	Event	Magnitude	PGA, g		Hypocentral distance (km)	Site Geology:	Location
			Direction 1	Direction 2			
1	Chamoli Aftershock 1999-03-29 08:49:45 UTC	4.6	0.1	0.11	24.6	Rock	Gopeshwar, India
2	Chamoli 1999-03-28 19:05:11 UTC	6.6	0.16	0.22	123.7	Rock	Barkot, India
3	Chamba 1995-03-24 11:52:33 UTC	4.9	0.24	0.29	37.5	Rock	Rakh, India
4	India-Burma Border 1995-05-06 01:59:07 UTC	6.4	0.3	0.42	261.9	Soil	Haflong, India
5	India-Burma Border 1987-05-18 01:53:51 UTC	5.9	0.46	0.39	155	Rock	Panimur, India
6	India-Burma Border 1990-01-09 18:51:29 UTC	6.1	0.55	0.6	233.5	Rock	Laisong, India
7	India-Bangladesh Border 1988-02-06 14:50:45 UTC	5.8	0.64	0.78	117.5	Rock	Khliehriat, India
8	Xizang-India Border 1996-03-26 08:30:25 UTC	4.8	0.76	0.37	49.9	Rock	Ukhimath, India
9	NE India 1986-09-10 07:50:26 UTC	4.5	0.88	0.87	50.9	Rock	Dauki, India
10	India-Burma Border 1988-08-06 00:36:25 UTC	7.2	0.96	0.9	206.5	Rock	Hajadisa, India
111	Bhuj/Kachchh 2001-01-26 03:16:40 UTC	7.0	1.03	0.9	239	N/A	Ahmedabad India
12	Uttarkashi 1991-10-19 21:23:15 UTC	7.0	1.15	1.16	39.3	Rock	Ghansiali, India
13	India-Burma Border 1997-05-08 02:53:15 UTC	5.6	1.48	0.93	65.4	Soil	Silchar, India

### 3.4 FRAGILITY CURVES USING COEFFICIENT BASED METHOD

According to the approach portrayed in previous segment fragility curves are produced utilizing coefficient based method for various performance levels. In the fragility analysis the demands of the structures are log normally distributed i.e. the demands and the IMs can be prophesied by a power model .The fragility curve which graphically signify the seismic risk of the structure, as the probability of exceeding prescribed damage state.

#### 3.4.1 Two Storey Buildings

A two storey two bay masonry infilled reinforced concrete building having storey height 3.2m and bay width 5m model is designed. The computational model is subjected to earthquake ground motion recorded in Table 3.1 and the fundamental time period to the structure is calculated according to the code *IS 1893*. The nonlinear dynamic analysis is performed on the structure to obtain the storey drift and periodic shift of the building for each value of PGA. All the data collected from the analysis are presented in the table 3.2 as follows:

**Table 3.2** Experimental data for 2-storey building

Number of stories(N)	model height	PGA in g	IDR( $\theta$ )	PSF( $\beta$ )
2	6.4	0.1	0.000177	1.059
2	6.4	0.16	0.000238	1.288
2	6.4	0.24	0.000541	1.274
2	6.4	0.3	0.001774	1.286
2	6.4	0.46	0.001703	1.304
2	6.4	0.55	0.002226	1.291
2	6.4	0.64	0.005523	1.298
2	6.4	0.76	0.002184	1.085
2	6.4	0.88	0.004563	1.069
2	6.4	0.96	0.006865	1.282
2	6.4	1.03	0.017116	1.066
2	6.4	1.15	0.011344	1.295
2	6.4	1.48	0.043	1.076



2	6.4	0.11	0.000286	1.062
2	6.4	0.22	0.001083	1.294
2	6.4	0.29	0.001259	1.090
2	6.4	0.42	0.001465	1.302
2	6.4	0.39	0.002104	1.069
2	6.4	0.6	0.002306	1.071
2	6.4	0.78	0.009249	1.063
2	6.4	0.37	0.000776	1.100
2	6.4	0.87	0.006681	1.113
2	6.4	0.9	0.004922	1.083
2	6.4	0.9	0.017685	1.075
2	6.4	1.16	0.008336	1.078
2	6.4	0.93	0.011992	1.099

#### 3.4.1.1 Relationship between inter-story drift ratio (IDR) with peak ground acceleration (PGA)

Scatter plots of the IDR as a function of PGA for two masonry infilled (RC) structures are indicated in Fig. 3.1 , in which best fitting linear regression equation (on a logarithmic scale) for the reinforced concrete structures are as follows:

$$\ln(\theta) = 1.7736 \times \ln(PGA) - 4.6897 \quad (3.1)$$

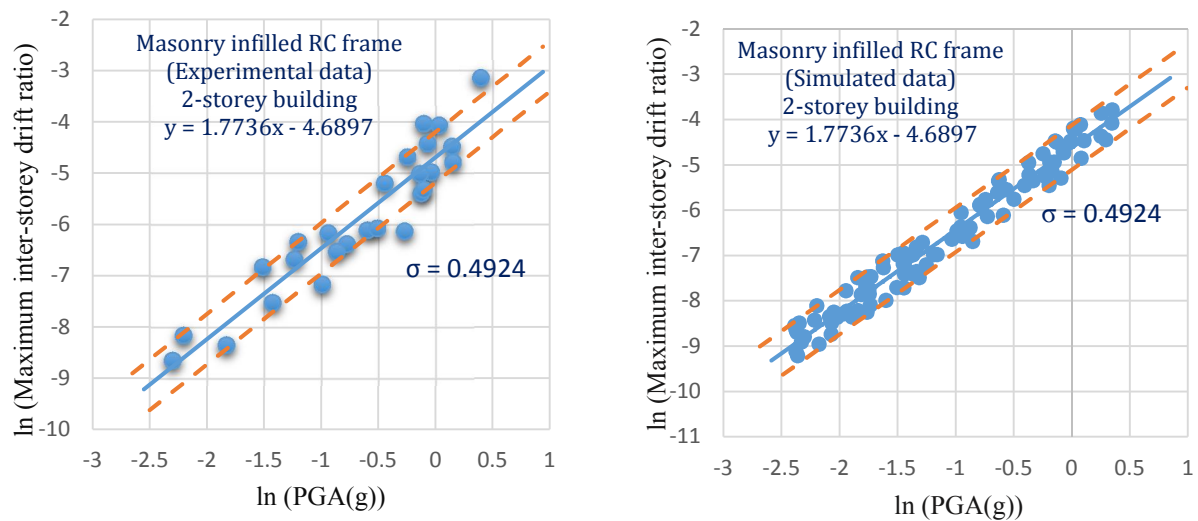


**Fig. 3.1** Variation of Inter-storey drift ratio (IDR) with peak ground Acceleration (PGA)

### 3.4.1.2 Relationship between period shift factor (PSF) with peak ground acceleration (PGA)

Similarly, Scatter plots of the PSF as a function of PGA for two story masonry infilled (RC) structures are indicated in Fig. 3.2, in which best fitting linear regression equation (on a logarithmic scale) for the reinforced concrete structures are as follows:

$$\ln(\beta) = -0.0206 \times \ln(\text{PGA}) + 0.6534 \quad (3.2)$$

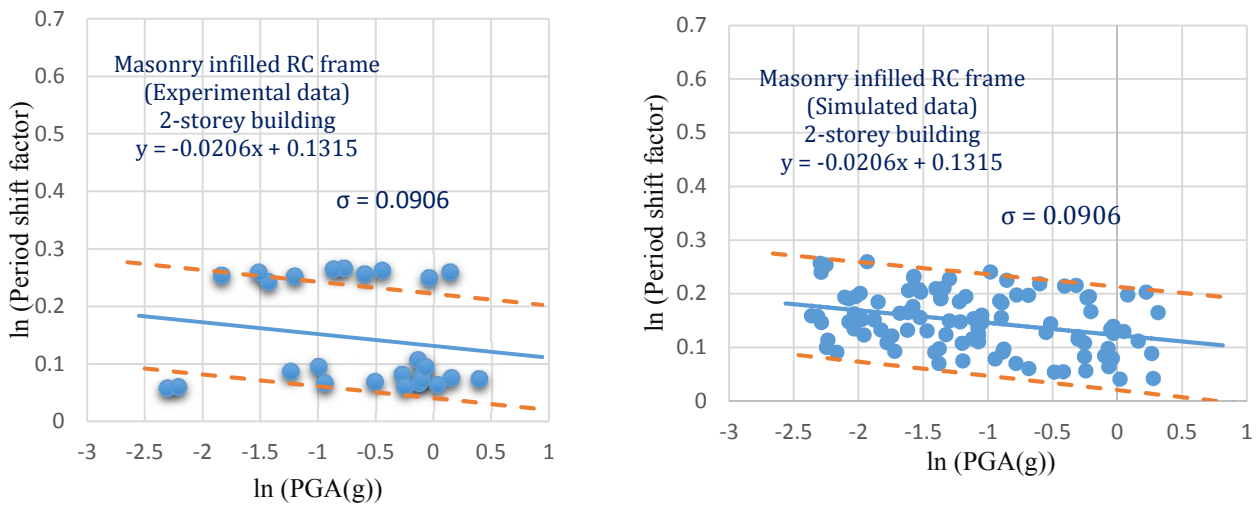


**Fig. 3.2** Variation of Period shift factor (PSF) with peak ground Acceleration (PGA)

To calibrate the drift factor ( $\lambda$ ) in this present study, the IDRs of  $\theta = 0.005, 0.01, 0.015$  and  $0.02$  are considered. From the IDR values the PGA can be calculated using Eq. 3.1 and also the period shift factors (PSF) of Masonry infilled RC structures corresponding to the predicted PGAs can also be obtained by using Eq. 3.2, summarized in Table 3.3. Using IS 1893 period–height formulas the fundamental period of structure for two storey masonry infilled RC structures with (a storey height of 3.2 m) is calculated and the drift factor ( $\lambda$ ) is also calculated from Eq. 2.17, the average drift factor  $\lambda=3.14$  is used to predict the spectral acceleration ( $S_a$ ) for the given IDR.

**Table 3.3** Coefficient based parameters obtained from regression equation ( $\lambda=3.14$ )

IDR( $\theta$ )	PGA in g	PSF( $\beta$ )	S <sub>a</sub> in g
0.005	0.71	1.14	0.94
0.01	1.04	1.1	1.90
0.015	1.32	1.13	2.88
0.02	1.55	1.13	3.87

### 3.4.2 Four Storey Buildings

A four storey two bay masonry infilled reinforced concrete building having storey height 3.2m and bay width 5m model is designed. The computational model is subjected to earthquake ground motion recorded in Table 3.1 and the fundamental time period to the structure is calculated according to the code IS 1893. The nonlinear dynamic analysis is performed on the structure to obtain the storey drift and periodic shift of the building for each value of PGA. All the data collected from the analysis are presented in the table 3.4 as follows:

**Table 3.4** Experimental data for 4-storey building

Number of stories( $N$ )	model height	PGA in g	IDR( $\theta$ )	PSF( $\beta$ )
4	12.8	0.1	0.00071	1.235
4	12.8	0.16	0.000545	1.198
4	12.8	0.24	0.0004	1.168
4	12.8	0.3	0.001114	1.194
4	12.8	0.46	0.001281	1.389
4	12.8	0.55	0.002324	1.206
4	12.8	0.64	0.004921	1.220
4	12.8	0.76	0.002515	1.290
4	12.8	0.88	0.004139	1.256
4	12.8	0.96	0.00567	1.187
4	12.8	1.03	0.032793	1.249
4	12.8	1.15	0.014434	1.214
4	12.8	1.48	0.060039	1.435
4	12.8	0.11	0.00051	1.239
4	12.8	0.22	0.001748	1.212
4	12.8	0.29	0.0012	1.301
4	12.8	0.42	0.001517	1.224

4	12.8	0.39	0.001351	1.254
4	12.8	0.6	0.002591	1.422
4	12.8	0.78	0.007044	1.401
4	12.8	0.37	0.001795	1.497
4	12.8	0.87	0.002648	1.528
4	12.8	0.9	0.006674	1.286
4	12.8	0.9	0.029125	1.267
4	12.8	1.16	0.011282	1.275
4	12.8	0.93	0.019196	1.321

### 3.4.2.1 Relationship between inter-story drift ratio (IDR) with peak ground acceleration (PGA)

Scatter plots of the IDR as a function of PGA for four storey masonry infilled RC structures are indicated in Fig. 3.3, in which best fitting linear regression equation (on a logarithmic scale) for the reinforced concrete structures are as follows:

$$\ln(\theta) = 1.5629 \times \ln(\text{PGA}) - 4.6717 \quad (3.3)$$

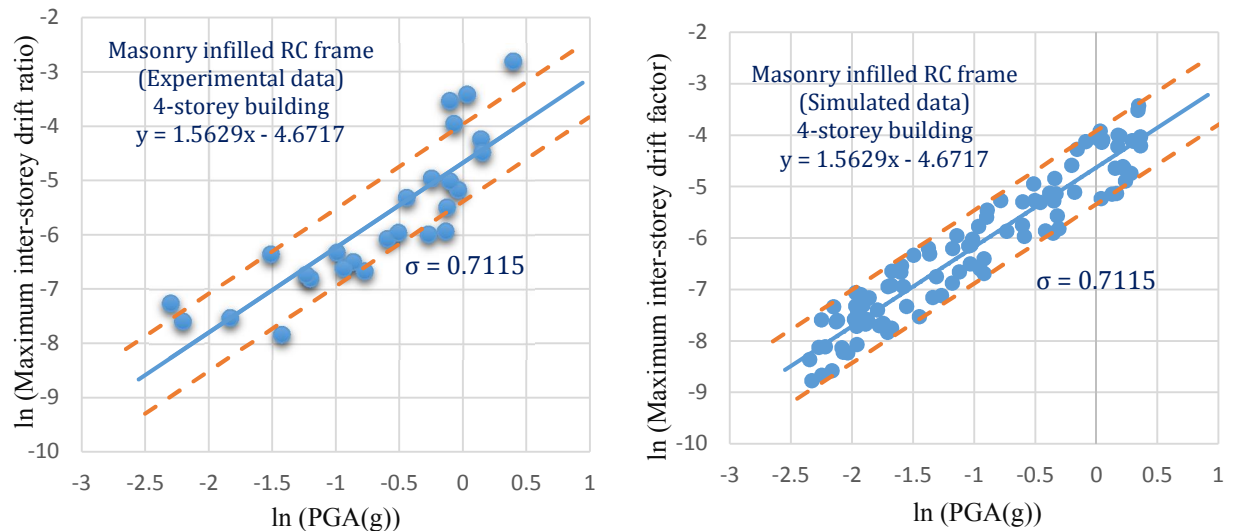


**Fig. 3.3** Variation of Inter-storey drift ratio (IDR) with peak ground Acceleration (PGA)

### 3.4.2.2 Relationship between period shift factor (PSF) with peak ground acceleration (PGA)

Similarly, Scatter plots of the PSF as a function of PGA for masonry infilled RC structures are indicated in Fig. 3.4, in which best fitting linear regression equation (on a logarithmic scale) for the reinforced concrete structures are as follows:

$$\ln(\beta) = 0.0317 \times \ln(\text{PGA}) + 0.2712 \quad (3.4)$$

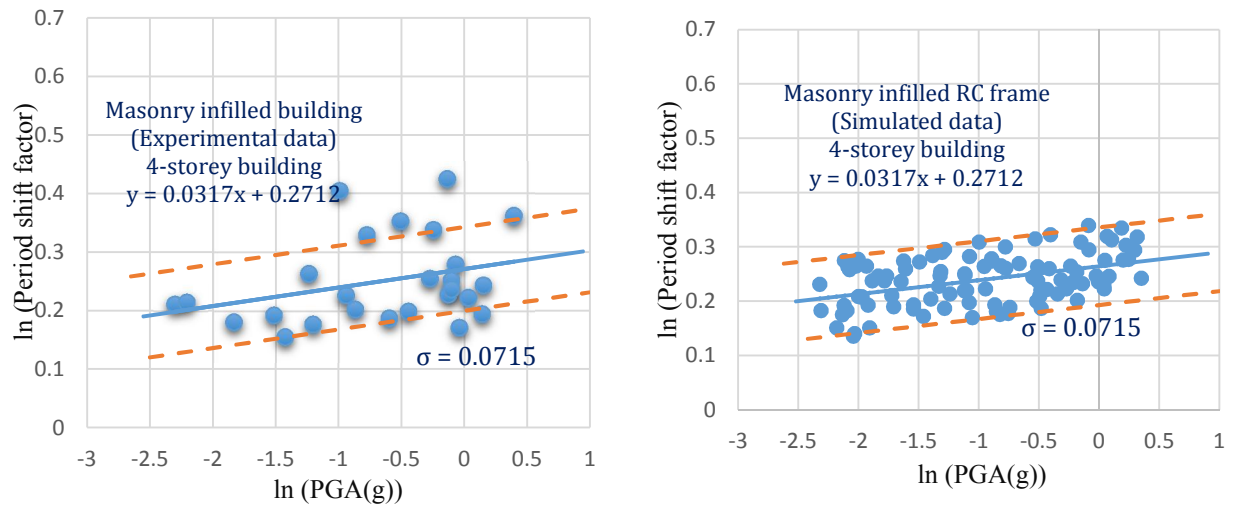


**Fig. 3.4** Variation of Period shift factor (PSF) with peak ground Acceleration (PGA)

To calibrate the drift factor ( $\lambda$ ) in this present study, the IDRs of  $\theta = 0.005, 0.01, 0.015$  and  $0.02$  are considered. From the IDR values the PGA can be calculated using Eq. 3.3 and also the period shift factors (PSF) of masonry infilled RC structures corresponding to the predicted PGAs can also be obtained by using Eq. 3.4, summarized in Table 3.5. Using IS 1893 period–height formulas the fundamental period of structure for four storey masonry infilled RC structures with (a storey height of 3.2 m) is calculated and the drift factor ( $\lambda$ ) is also calculated from Eq. 2.17, the average drift factor  $\lambda=3.14$  is used to predict the spectral acceleration ( $S_a$ ) for the given IDR.

**Table 3.5** Coefficient based parameters obtained from regression equation ( $\lambda=3.14$ )

IDR( $\theta$ )	PGA in g	PSF( $\beta$ )	Sa in g
0.005	0.67	1.29	0.37
0.01	1.04	1.31	0.72
0.015	1.35	1.32	1.05
0.02	1.62	1.33	1.39

### 3.4.3 Six Storey Buildings

A six storey two bay masonry infilled reinforced concrete building having storey height 3.2m and bay width 5m model is designed. The computational model is subjected to earthquake ground motion recorded in Table 3.1 and the fundamental time period to the structure is calculated according to the code IS 1893. The nonlinear dynamic analysis is performed on the structure to obtain the storey drift and periodic shift of the building for each value of PGA. All the data collected from the analysis is presented in the table 3.6 as follows:

**Table 3.6** Experimental data for 6-storey building

Number of stories( $N$ )	model height	PGA in g	IDR( $\theta$ )	PSF( $\beta$ )
6	19.2	0.1	0.001087	1.473
6	19.2	0.16	0.000378	1.413
6	19.2	0.24	0.000521	1.275
6	19.2	0.3	0.00143	1.406
6	19.2	0.46	0.00241	1.491
6	19.2	0.55	0.001831	1.425
6	19.2	0.64	0.003734	1.449
6	19.2	0.76	0.002306	1.559
6	19.2	0.88	0.005491	1.501
6	19.2	0.96	0.005876	1.303
6	19.2	1.03	0.022006	1.497
6	19.2	1.15	0.013889	1.440
6	19.2	1.48	0.040988	1.526
6	19.2	0.11	0.00066	1.479
6	19.2	0.22	0.002356	1.342

6	19.2	0.29	0.001273	1.580
6	19.2	0.42	0.002571	1.455
6	19.2	0.39	0.003144	1.497
6	19.2	0.6	0.003266	1.507
6	19.2	0.78	0.007291	1.484
6	19.2	0.37	0.001186	1.621
6	19.2	0.87	0.004592	1.669
6	19.2	0.9	0.006744	1.553
6	19.2	0.9	0.023497	1.519
6	19.2	1.16	0.015033	1.534
6	19.2	0.93	0.014696	1.614

### 3.4.3.1 Relationship between inter-story drift ratio (IDR) with peak ground acceleration (PGA)

Scatter plots of the IDR as a function of PGA for six storey masonry infilled RC structures are indicated in Fig. 3.5, in which best fitting linear regression equation (on a logarithmic scale) for the reinforced concrete structures are as follows:

$$\ln(\theta) = 1.4242 \times \ln(\text{PGA}) - 4.6749 \quad (3.5)$$

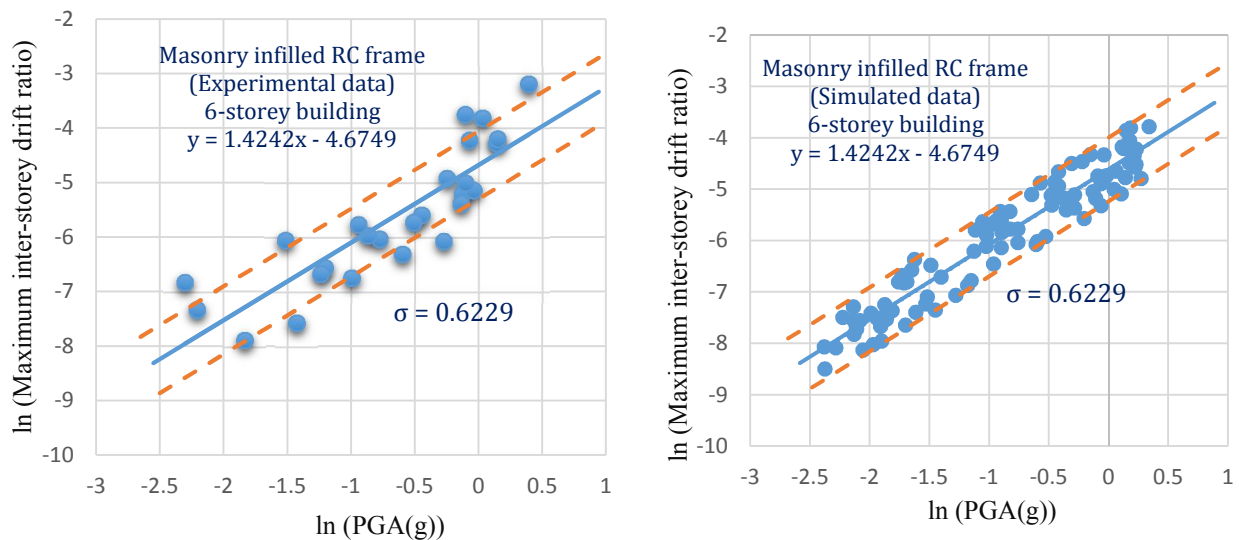


**Fig. 3.5** Variation of Inter-storey drift ratio (IDR) with peak ground Acceleration (PGA)

### 3.3.3.2 Relationship between period shift factor (PSF) with peak ground acceleration (PGA)

Similarly, Scatter plots of the PSF as a function of PGA for six storey masonry infilled RC structures are indicated in Fig. 3.6, in which best fitting linear regression equation (on a logarithmic scale) for the reinforced concrete structures are as follows:

$$\ln(\beta) = 0.0267 \times \ln(\text{PGA}) + 0.4115 \quad (3.6)$$

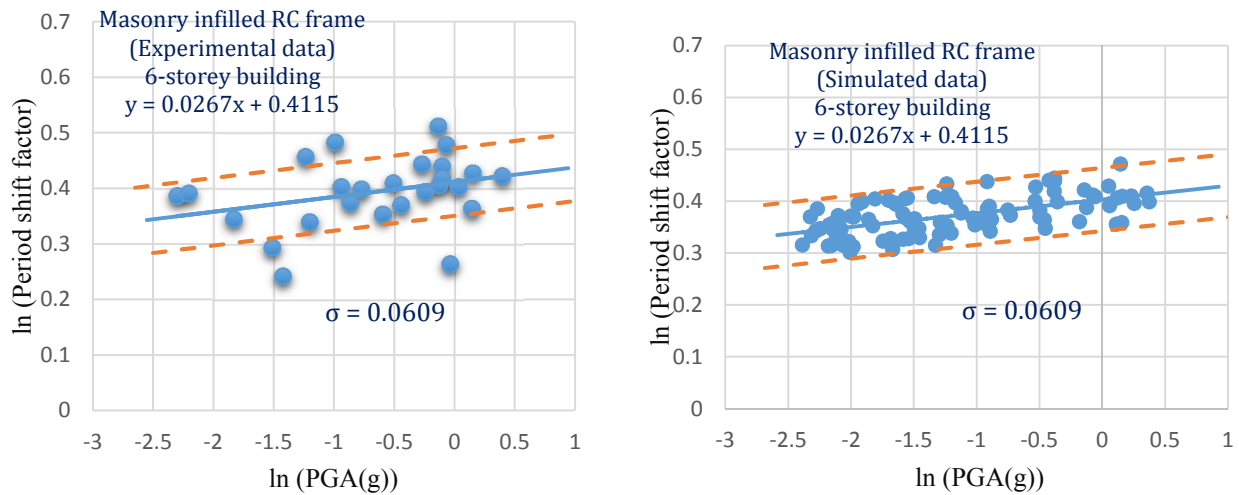


**Fig. 3.6** Variation of Period shift factor (PSF) with peak ground Acceleration (PGA)

To calibrate the drift factor ( $\lambda$ ) in this present study, the IDRs of  $\theta = 0.005, 0.01, 0.015$  and  $0.02$  are considered. From the IDR values the PGA can be calculated using Eq. 3.5 and also the period shift factors (PSF) of masonry infilled reinforced concrete structures corresponding to the predicted PGAs can also be obtained by using Eq. 3.6, summarized in Table 3.7. Using IS 1893 period–height formulas the fundamental period of structure for six storey MI RC buildings with (a storey height of 3.2 m) is calculated and the drift factor ( $\lambda$ ) is also calculated from Eq. 2.17, the average drift factor  $\lambda=3.14$  is used to predict the spectral acceleration ( $S_a$ ) for the given IDR.



**Table 3.7** Coefficient based parameters obtained from regression equation ( $\lambda=3.14$ )

IDR( $\theta$ )	PGA in g	PSF( $\beta$ )	Sa in g
0.005	0.64	1.49	0.18
0.01	1.05	1.51	0.36
0.015	1.39	1.52	0.53
0.02	1.71	1.53	0.70

#### 3.4.4 Spectral acceleration ( $S_a$ ) based fragility curve by the coefficient-based method

Fragility curves in terms of spectral acceleration ( $S_a$ ) for masonry infilled RC structures were built utilizing the coefficient-based methodology. Spectral acceleration based fragility curve that graphically represent the seismic risk of structure used for seismic performance evaluation and seismic vulnerability assessment of building. FEMA-356 (ASCE, 2000) specified damage states of RC structures immediate occupancy (*IO*), life safety (*LS*) and collapse prevention (*CP*) state. The damage states can be represented by the specific inter-storey drift limits of 1%, 2%, and 4% for immediate occupancy (*IO*), life safety (*LS*) and collapse prevention (*CP*) state respectively (ASCE, 2000). These proposed limits are considered if the buildings are appropriately intended for seismic loading but for old buildings and buildings with a gravity-load design due to inadequate column strength and segment detailing diminished drift limits to 0.5%, 1%, and 2%. The spectral acceleration based fragility curves for masonry infilled RC structures with various number of stories for different performance levels are shown in Fig. 3.7, 3.8 and 3.9.

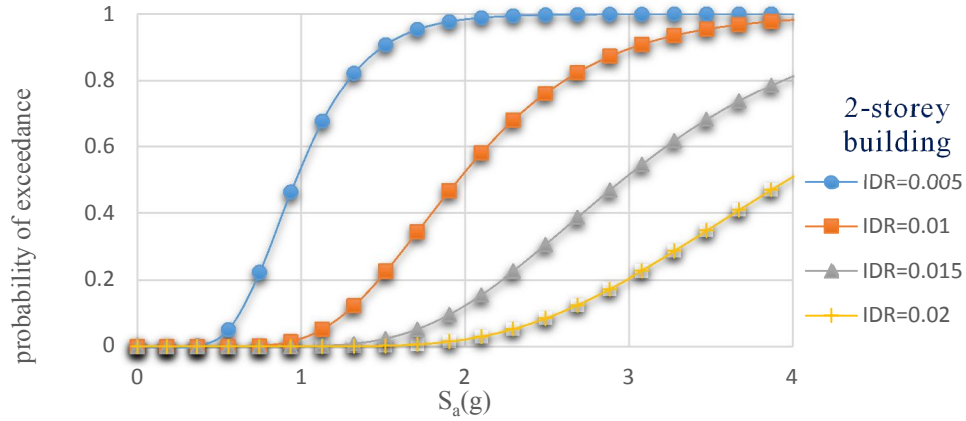


**Fig. 3.7** Spectral acceleration based fragility curve for two storey MI RC buildings

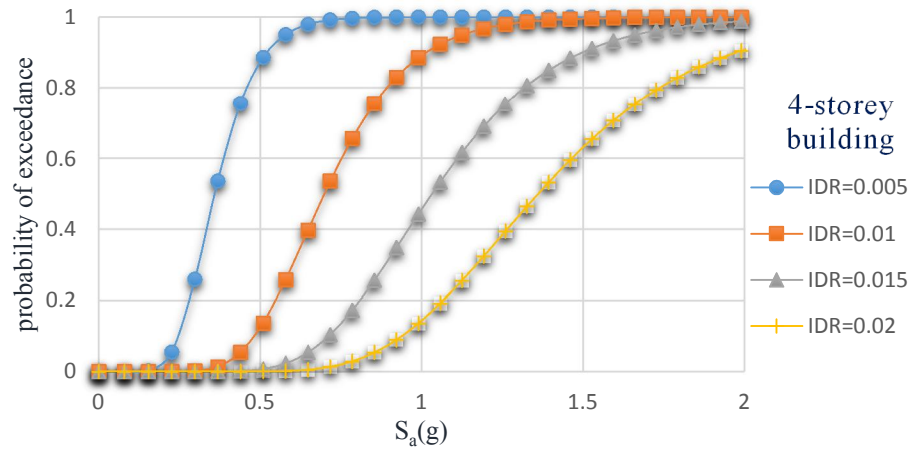


**Fig. 3.8** Spectral acceleration based fragility curve for four storey MI RC buildings

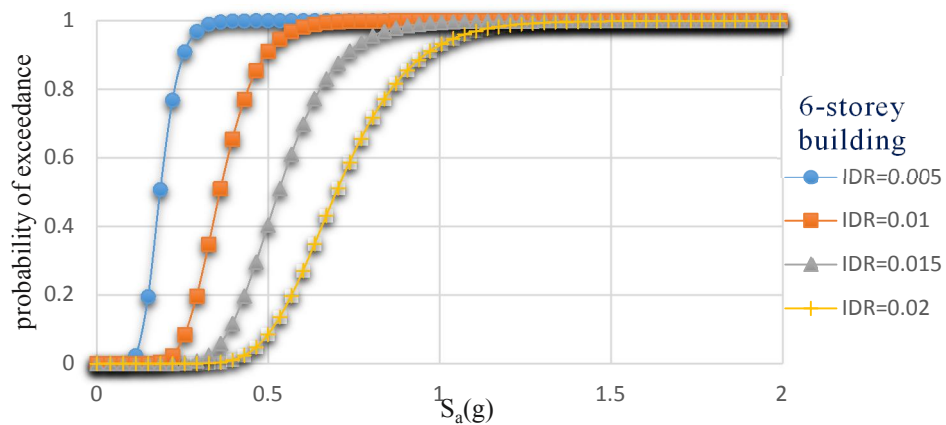


**Fig. 3.9** Spectral acceleration based fragility curve for six storey MI RC buildings

The spectral acceleration based fragility curves for masonry infilled reinforced concrete buildings with various number of stories under different performance levels are shown in Fig. 3.10 in which number of stories has a significant effect on the fragility curve, with increase in the number of stories the probability of exceedance increases for a specified performance level (for *IO*, *LS* and *CP* state) of two, four and six storey masonry infilled (MI) reinforced concrete (RC) building.

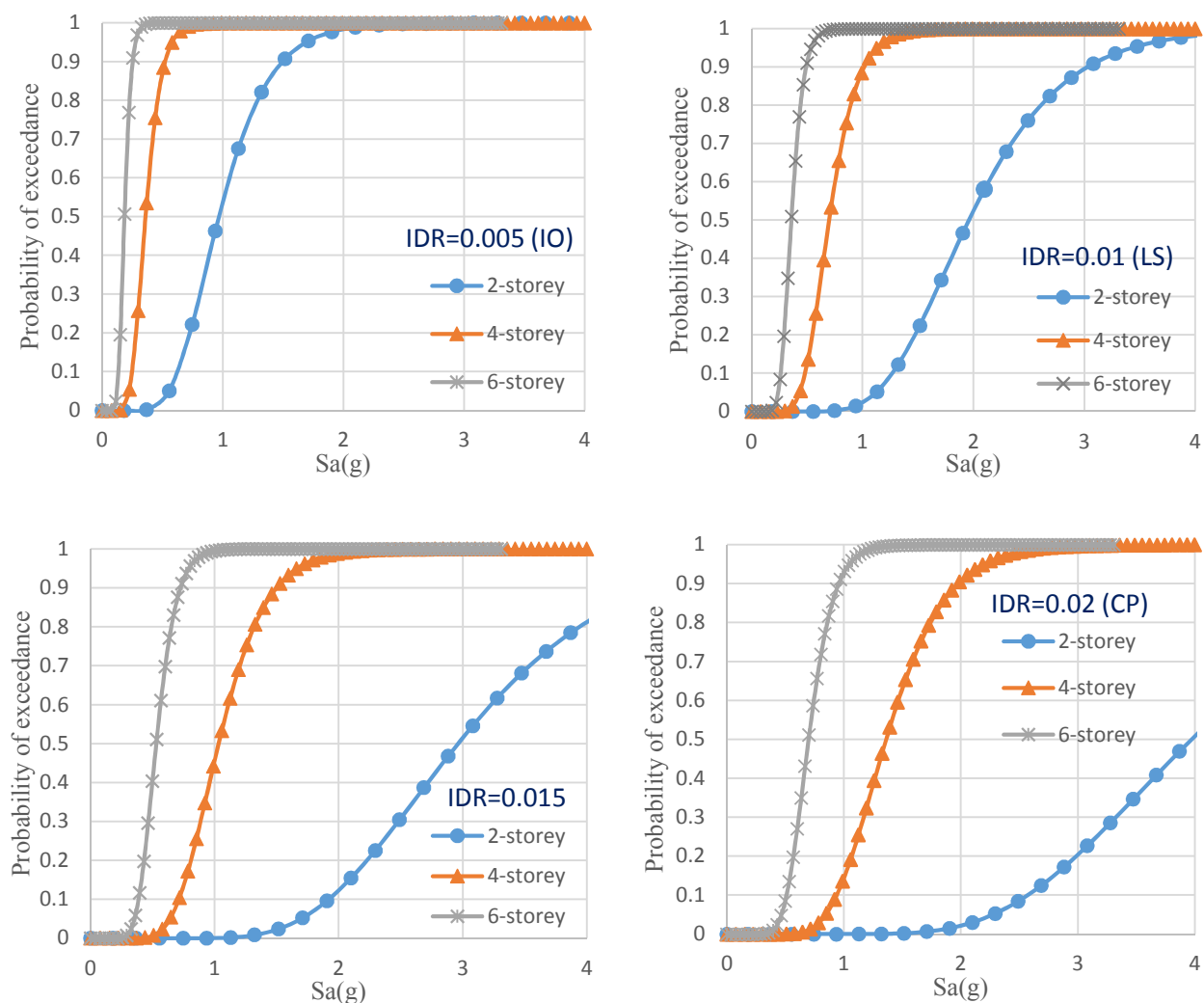


**Fig. 3.10** Spectral acceleration based fragility curve of MI RC buildings for various performance levels

The spectral acceleration based fragility curve are shown in the Fig. 3.7,3.8 and 3.9 respectively for various performance level and various number of stories. The median spectral accelerations (with 50% fragility or 50% exceedance) for two, four, six storey masonry infilled (MI) reinforced concrete (RC) buildings are 0.97g, 0.36g, 0.18g for the IO state (IDR=0.005); 1.96g, 0.70g, 0.36g for the LS state (IDR=0.01); and 3.97g, 1.36g, 0.70g for the CP state (IDR=0.02) respectively are shown in Fig. 3.11, 3.12 and 3.13.

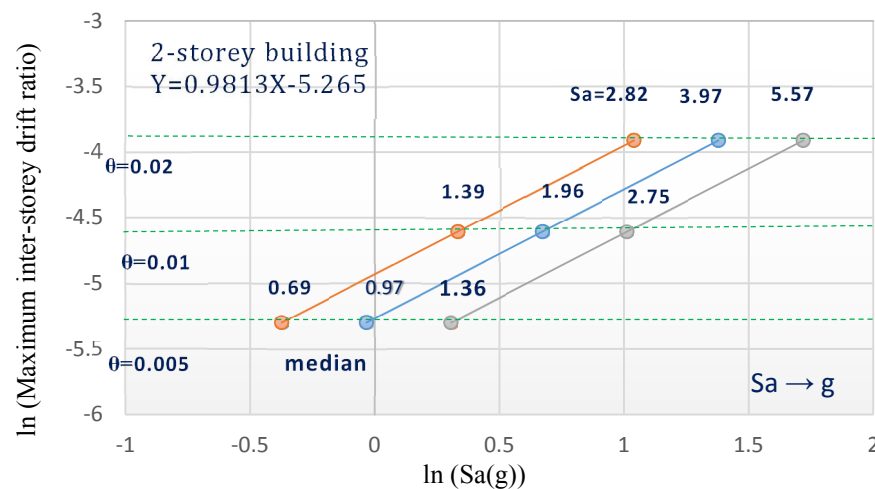


**Fig. 3.11** spectral acceleration for two storey MI RC building corresponding to inter storey drift ratio of 0.005, 0.01 and 0.02

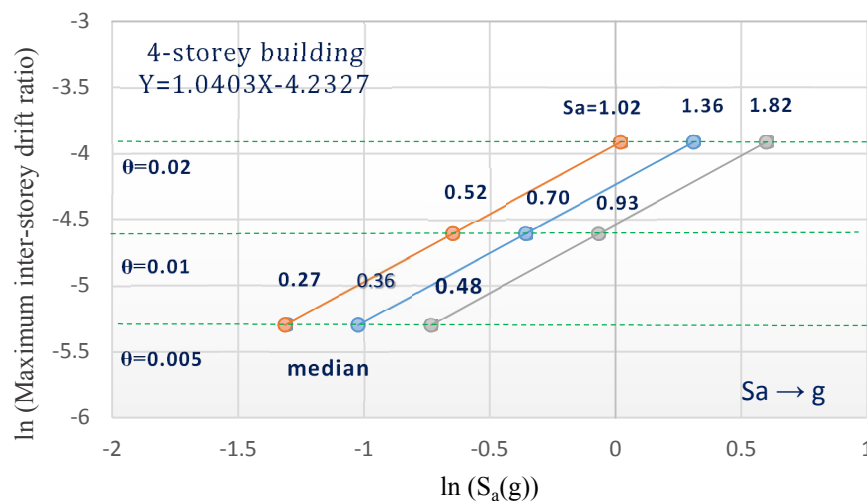


**Fig. 3.12** spectral acceleration for four storey MI RC building corresponding to inter storey drift ratio of 0.005, 0.01 and 0.02

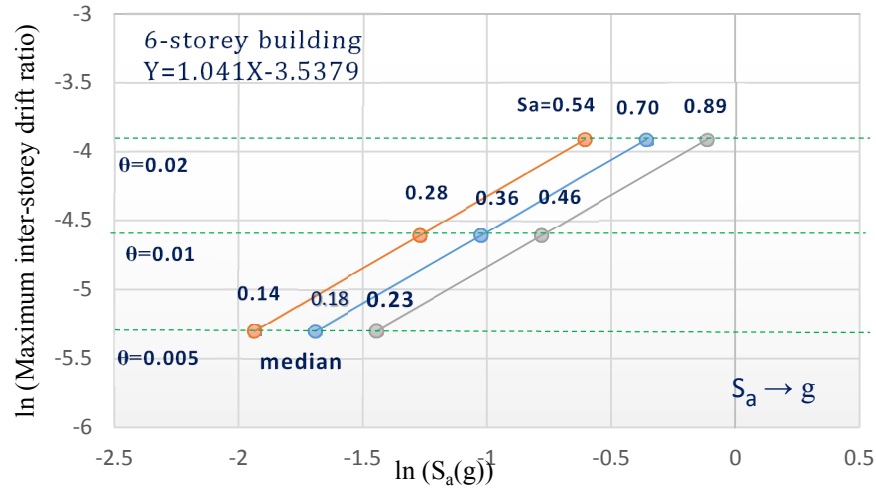


**Fig. 3.13** spectral acceleration for six storey MI RC building corresponding to inter storey drift ratio of 0.005, 0.01 and 0.02

### 3.4.5 Spectral displacement ( $S_d$ ) based fragility curve by the coefficient-based method

Spectral displacement based fragility curve is opposed to spectral acceleration based fragility curve, is an alternative path for evaluating seismic performance of the buildings. The fragility curve for masonry infilled reinforced concrete structures at the damage state of 0.5%, 1%, 2% (IO, LS, and CP performance levels) in terms of IDR are constructed in this study are shown in Fig. 3.14, 3.15 and 3.16

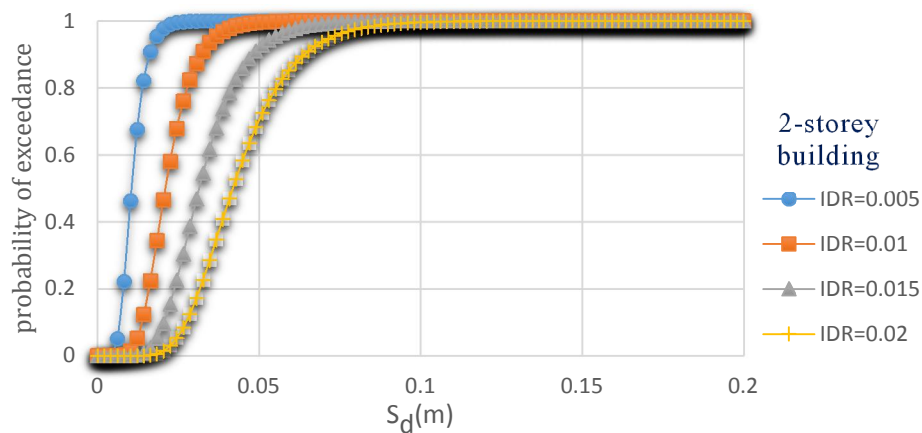


**Fig. 3.14** Spectral displacement based fragility curve for two storey MI RC buildings for various performance level

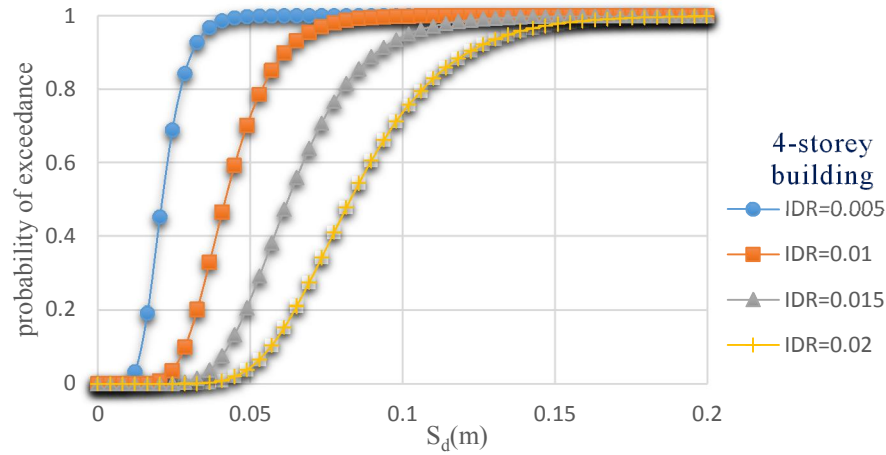


**Fig. 3.15** Spectral displacement based fragility curve for four storey MI RC buildings for various performance level

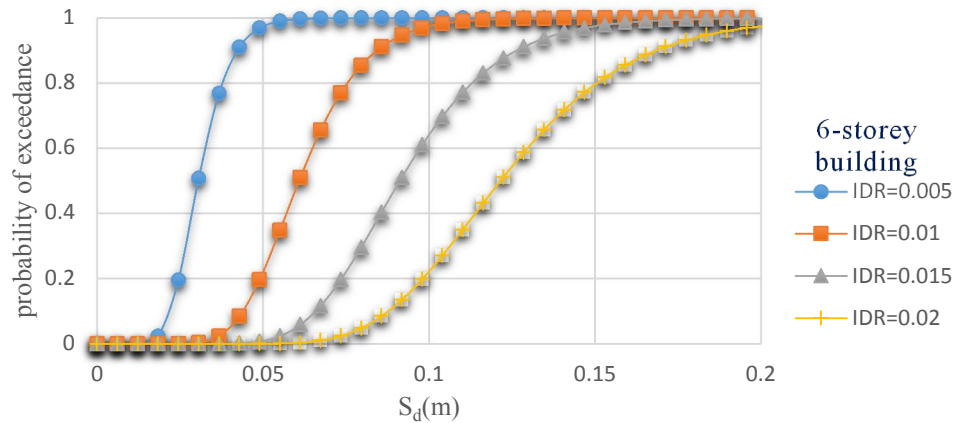


**Fig. 3.16** Spectral displacement based fragility curve for six storey MI RC buildings for various performance level

The spectral displacement based fragility curve are shown in the Fig. 3.14, 3.15 and 3.16 for various performance level and various number of stories. The median spectral displacement (with 50% fragility or 50% exceedance) for two, four, six storey masonry infilled (MI) reinforced concrete (RC) buildings are 1.05 cm, 2.11 cm, 3.04 cm for the IO state (IDR=0.005); 2.09 cm, 4.19 cm, 6.08 cm for the LS state (IDR=0.01); and 4.18 cm, 8.29 cm, 12.15 cm for the CP state (IDR=0.02) respectively are shown in Fig. 3.17, 3.18 and 3.19.

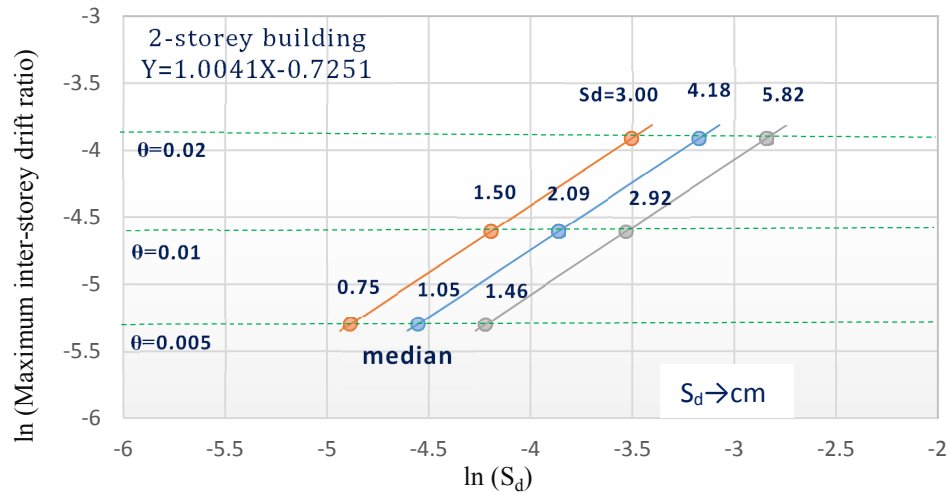


**Fig. 3.17** spectral displacement for two storey MI RC building corresponding to inter storey drift ratio of 0.005, 0.01 and 0.02

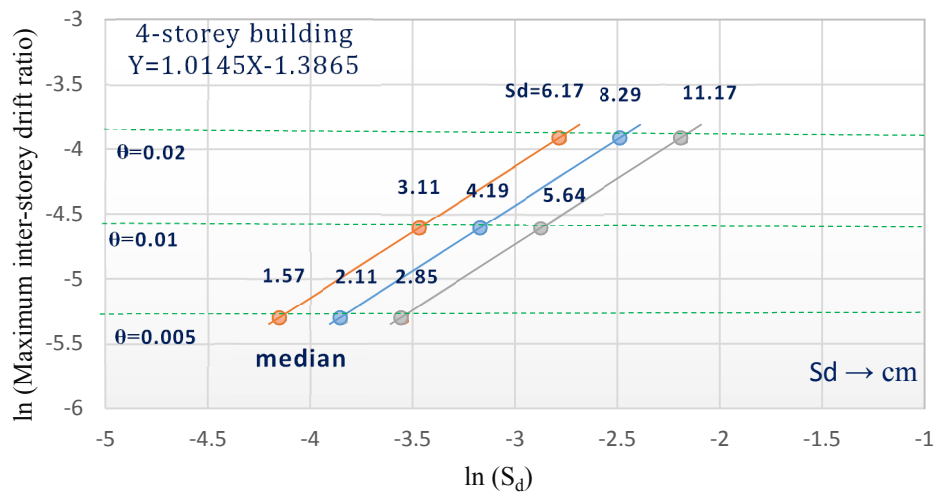


**Fig. 3.18** spectral displacement for four storey MI RC building corresponding to inter storey drift ratio of 0.005, 0.01 and 0.02

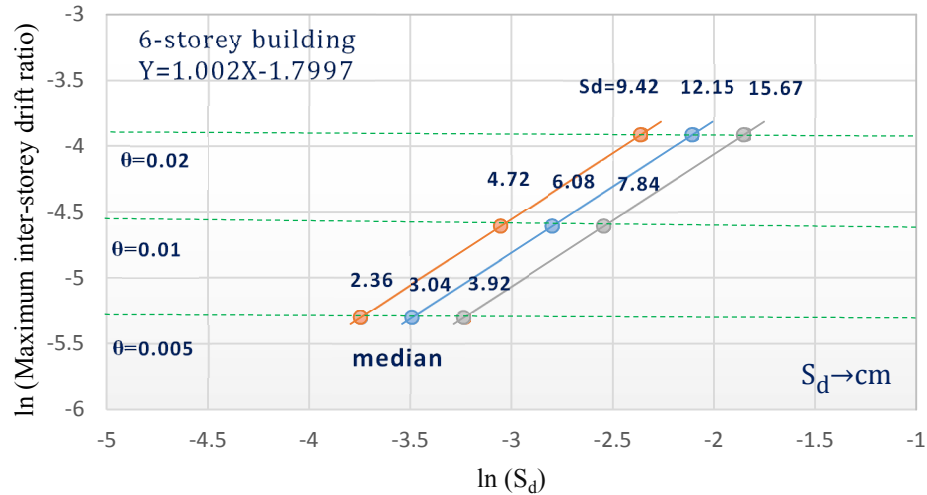


**Fig. 3.19** spectral displacement for six storey MI RC building corresponding to inter storey drift ratio of 0.005, 0.01 and 0.02

### 3.4.6 Comparison of fragility curve by coefficient based method and SAC FEMA method at the collapse state

The fragility curves for masonry infilled RC structures in terms of PGA with various number of stories at the CP state performance levels are plotted for both the coefficient based method and SAC FEMA method are shown in Fig. 3.20, 3.21 and 3.22. The fragility curve for two, four, six storey building obtained from coefficient based method and SAC FEMA method are compared in Fig. 3.20, 3.21 and 3.22, and it can be seen that the results are correspond well. The slight variation of fragility curves in both the methods is mainly due to Uncertainty in dispersions demand ( $\beta_c$ ,  $\beta_{d/IM}$ ,  $\beta_M$ ) i.e.  $\beta_c$  the uncertainty in building definition and construction quality,  $\beta_M$  the uncertainty in component modelling, damping and mass assumption and  $\beta_q$  due to the behavior of structure and study of component deterioration and failure mechanism consider in SAC FEMA method.



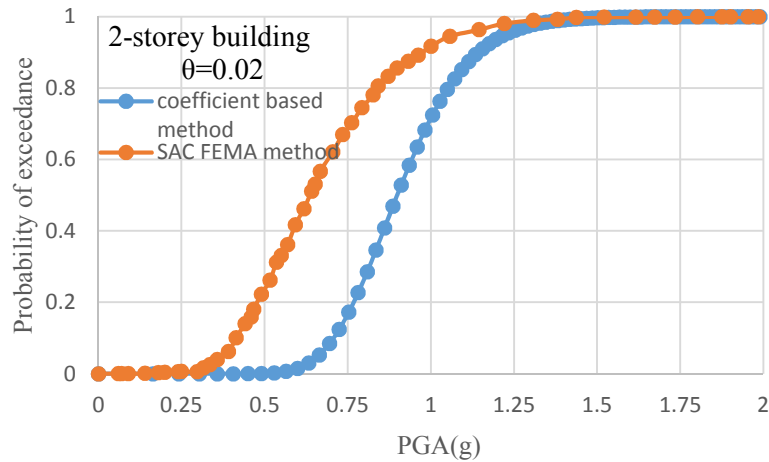


**Fig. 3.20** Comparison of fragility curve of two storey MI RC buildings at the CP state (IDR=0.2%)

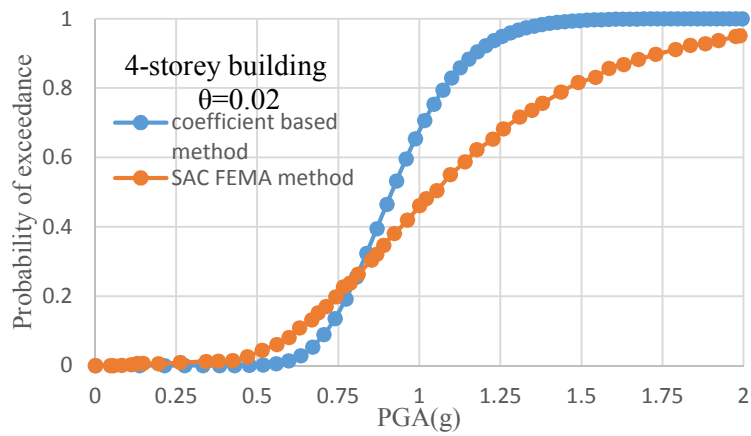


**Fig. 3.21** Comparison of fragility curve of four storey MI RC buildings at the CP state (IDR=0.2%)

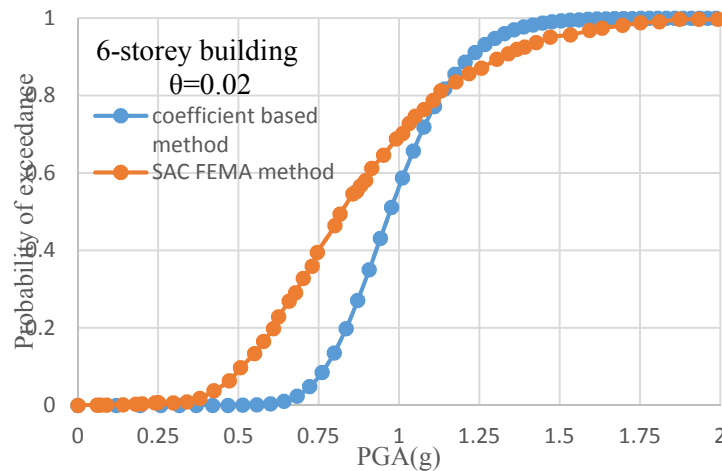


**Fig. 3.22** Comparison of fragility curve of six storey MI RC buildings at the CP state (IDR=0.2%)

### 3.5 SUMMARY

This chapter detail discussed about the fragility curve for two, four and six storey masonry infilled reinforced concrete buildings using coefficient based method. This chapter started with the selecting ground motion data from different region from past earthquake in India from CESMD website. The computational model of two, four and six storey building is subjected to earthquake ground motion recorded in Table 3.1 and nonlinear dynamic analysis is performed on the to obtain the inter storey drift ratio and the period shift (or the stiffness deterioration) of the building. Using lognormal distribution the interrelation between coefficient based parameters are obtained to calculate the spectral displacement and spectral acceleration at the different performance level of drift limit 0.5%,1% and 2%.

The spectral acceleration and spectral displacement based fragility curves are plotted of masonry infilled reinforced concrete buildings for probability of exceeding various damage state or performance level (IDR of 0.5%, 1% and 2%) and various number of stories (two, four and six storey) buildings using coefficient based method. The fragility curve that graphically represent the seismic risk of structure used for seismic performance evaluation and seismic vulnerability assessment of building. Finally, the fragility curves for masonry infilled reinforced concrete buildings with various number of stories at the CP state (IDR=0.2%) performance levels are compared for both the coefficient based method and SAC FEMA method and the comparison results are correspond well for estimating the seismic risk of the structure.

#### 4.1 SUMMARY

The main goals of this study are to estimate seismic vulnerability of masonry in filled reinforced concrete structures through seismic fragility analysis and to assess the seismic risk of a structure.

To achieve the desire objective the problem is being divided into different sub parts:

- Validate and Develop fragility curves of Typical RC frames with number of stories ranging from two to six stories using coefficient based method (Method I) proposed by Lee and Su (2012)
- Development of seismic fragility curves for the same frames based on SAC FEMA method (Method II).
- A critical comparison of the fragility curves between two methods (Method I and II).

To achieve the above desire objectives, an extensive literature review is carried out on following area are (a) the various methodologies for the seismic vulnerability assessment of masonry infilled reinforced concrete buildings as per various international codes and literatures, (b) study of the building performance level or (the Damage States) of the building and (c) fragility curves on masonry infilled (MI) reinforced concrete (RC) framed buildings using coefficient based method (Lee and Su, 2012) and SAC FEMA method (Cornell *et al.*, 2002).

The chapter 2 presents the detailed procedure of seismic risk assessment in a probabilistic framework using lognormal distribution and briefly explains the coefficient based method and

SAC FEMA method used in the present study to obtain the fragility curves for the buildings. The validation study of coefficient based method using published experimental shaking table test results obtained for different storey buildings.

This ground motion data is selected from different region from past earthquake in India from CESMD website. The computer based model of two, four and six storey building are design by and the building model subjected to receded earthquake ground motion intensity. Nonlinear dynamic analyses is carried out to the model to obtain the inter storey drift ratio and the period shift (or the stiffness deterioration) of the building. The spectral acceleration and spectral displacement based fragility curves for two, four and six storey masonry infilled reinforced concrete buildings are plotted using coefficient based method. Finally, the fragility curves for masonry infilled reinforced concrete buildings at the damage state for both the coefficient based method and SAC FEMA methods are compared.

## **4.2 CONCLUDING REMARKS**

This study proposed the coefficient based method for seismic fragility analysis of masonry infilled reinforced concrete building, for selected ground motion intensity in rock or soil condition in different region from past earthquakes in India. The coefficient based method is a simplified technique without finite element analysis for estimating the spectral acceleration and spectral acceleration demand of the structure. The spectral acceleration and displacement fragility curves are plotted for various number of stories and various performance level for specified damage state of inter storey drift ratio of 0.5%, 1% and 2% by coefficient based method. The fragility curves for masonry infilled (MI) reinforced concrete (RC) building at the collapse state obtained from coefficient based method is compared with SAC FEMA method.

The fragility curves obtained can provide a good vulnerability assessment for masonry infilled reinforced concrete buildings at different damage state performance level.

Based on the results and analyses the following conclusion are obtained:

- 1) The spectral acceleration and spectral displacement for two, four and six storey masonry infilled reinforced concrete building are obtained using regression analyses and coefficient based parameters such as IDR and PSF are calculated from PGA values and the drift factor predicted from Eq. 2.17 as  $\lambda=3.14$ .
- 2) The spectral acceleration and spectral displacement based fragility curves for two, four and six storey masonry infilled reinforced concrete building for various performance level are obtained using coefficient based method and median, lower bound and upper bound spectral acceleration and displacement are calculated for inter-storey drift ratio of 0.5%, 1% and 2%. The fragility curves achieved can afford a satisfactory vulnerability assessment of buildings for different damage state performance level.
- 3) The fragility curves obtained from coefficient based method is compared with SAC FEMA method at the damage state (CP state) and a good correlation is obtained for both the method for evaluating seismic performance of building

### **4.3 LIMITATION OF PRESENT STUDY AND SCOPE OF FUTURE WORK**

The present study is limited to masonry infilled reinforced concrete buildings up to six-storey that are regular in plan and plan asymmetry arising from infill walls are not considered in the analysis. This study can be extended for bare frame building and open ground storey (OGS) buildings for multi-storey frame structures.

Only the spectral acceleration and displacement fragility curves are obtained using coefficient based method in this study. Also Reliability curves can be developed for the masonry infilled reinforced concrete building for the seismic hazard determination using this method.

## REFERENCES

---

1. Akkar S, Sucuoglu H and Yakut A (2005). Displacement-based Fragility Functions for Low- and Mid-rise Ordinary Concrete Buildings, *Earthquake Spectra*, 21(4): 901–927.
2. ASCE (2000). American Society of Civil Engineers, *Prestandard and Commentary for the Seismic Rehabilitation of Buildings* (Report No. FEMA-356), Washington, D.C.
3. ATC (1996). Applied Technology Council, *Seismic Evaluation and Retrofit of Concrete Buildings* (ATC-40), Redwood City, California.
4. Barbat A, Moya Y and Canas J (1996). Damage Scenarios Simulation for seismic risk assessment in urban zones, *Earthquake Spectra*, 12(3):371-394.
5. Calvi GM, Pinho R, Magenes G, Bommer JJ, Restrepo-Velez LF and Crowley H (2006). Development of seismic vulnerability assessment methodologies over the past 30 years, *Journal of Earthquake Technology*, 472(3): 75-104.
6. Casciati F and Faravelli L (1991). *Fragility Analysis of Complex Structural Systems*, Research Studies Press, England.
7. Chandler, AM, Su, RKL and Lee, PKK (2002a). Seismic Drift Assessment for Hong Kong Buildings. Recent Developments in Earthquake Engineering, Annual Seminar 2001/02, the Hong Kong Institution of Engineers Structural Division and the Institution of Structural Engineers (HK Division), 17: 1-15.
8. Chandler, AM, Su, RKL and Sheikh, MN (2002b). Drift Based Seismic Assessment of Buildings in Hong Kong, Proceedings of International Conference on Advances and New Challenges in Earthquake Engineering Research (ICANCEER 2002), 15-20 August, Harbin and Hong Kong, CHINA, 3: 257-265.
9. Choi E, DesRoches R and Nielson B (2004). Seismic Fragility of Typical Bridges in Moderate Seismic Zones, *Engineering Structures*, 26(2): 187–199.
10. Chopra AK and Goel RK (1999). Capacity-demand Diagram Methods for Estimating Seismic Deformation of Inelastic Structures: SDF System, Report No. PEER-

1999/02(Pacific Earthquake Engineering Research Center), University of California, Berkeley.

11. Chopra AK and Goel RK (2002). A Modal Pushover Analysis Procedure for Estimating Seismic Demands for Buildings, *Earthquake Engineering and Structural Dynamics*, 31(3): 561–582.
12. Cornell CA, Jalayer F, Hamburger RO and Foutch DA (2002). Probabilistic Basis for 2000 SAC Federal Emergency Management Agency steel moment frame guidelines, *Journal of Structural Engineering*, ASCE, 128(4): 526–533.
13. Dumova-Jovanoska E (2000). Fragility curves for reinforced concrete structures in Scopje region, *Soil Dynamics and Earthquake Engineering* 19(6): 455-466.
14. Ellingwood RR, Celik OC and Kinali K (2007). Fragility Assessment of Building Structural Systems in Mid-America, *Earthquake Engineering and Structural Dynamics*, 36(13): 1935–1952.
15. Erberik MA and Elnashai AS (2004). Vulnerability analysis of flat slab structures”, 13th Word Conference on Earthquake Engineering, Vancouver, B.C, Canada, Paper No. 3102.
16. Fajfar P (2000). A Nonlinear Analysis Method for Performance-based Seismic Design, *Earthquake Spectra*, 16(3): 573–592.
17. Goulet CA, Haselton CB, Mitrani-Reiser J, Beck JL, Deierlein GG, Porter KA and Stewart JP (2007). Evaluation of the Seismic Performance of a Codeconfirming Reinforced-concrete Frame Building-from Seismic Hazard to Collapse Safety and Economic Losses, *Earthquake Engineering and Structural Dynamics*, 36(13): 1973–1997.
18. Gupta M and Krawinkler H (2000). Estimation of Seismic Drift Demands for Frame Structures, *Earthquake Engineering and Structural Dynamics*, 29(9): 1287–1305.
19. Han SW and Chopra AK (2006). Approximate Incremental Dynamic Analysis Using Modal Pushover Analysis Procedure, *Earthquake Engineering and Structural Dynamics*, 35(15): 1853–1873.
20. Kalkan E and Kunnath SK (2007). Assessment of Current Nonlinear Static Procedures for Seismic Evaluation of Buildings, *Engineering Structures*, 29(3): 305–316.



21. Kappos AJ, Panagopoulos G, Panagiotopoulos Cand Penelis G (2006). A hybrid method for the vulnerability assessment of R/C and URM buildings, *Bull Earthquake Engineering*, 4:391-413.
22. Kircil MS and Polat Z (2006). Fragility Analysis of Mid-rise R/C Frame Buildings, *Engineering Structures*, 28(9): 1335–1345.
23. Konstantinidis D and Makris N (2009). Experimental and Analytical Studies on the Response of Freestanding Laboratory Equipment to Earthquake Shaking, *Earthquake Engineering and Structural Dynamics*, 38(6): 827–848
24. Lagaros ND (2008). Probabilistic Fragility Analysis: A Tool for Assessing Design Rules of RC Buildings, *Earthquake Engineering and Engineering Vibration*, 7(1): 45–56.
25. Lang K and Bachmann H (2004). On the Seismic Vulnerability of Existing Buildings: A Case Study of the City of Basel, *Earthquake Spectra*, 20(1): 43–66.
26. Lee CL and Su RKL (2012). Fragility Analysis of Lowrise Masonry Infilled Reinforced Concrete Buildings by A Coefficient-based Spectral Acceleration Method, *Earthquake Engineering and Structural Dynamics*, 41(4): 697–713.
27. Lu Y, Gu X and Wei J (2009), Prediction of Seismic Drifts in Multi-story Frames with A New Story Capacity Factor, *Engineering Structures*, 31(2): 345–357.
28. Miranda E (1999). Approximate Seismic Lateral Deformation Demands in Multistory Buildings,” *Journal of Structural Engineering*, ASCE, 125(4): 417–425.
29. Moghaddam, HA, and Dowling, PJ, 1987. The State of the Art in Infilled Frames, ESEE Research Report No.87-2, Imperial College of Science and Technology, Civil Eng. Department, London, U.K.
30. Mosalam KM, Ayala G, White RN and Roth C (1997). Seismic Fragility of LRC Frames with and without Masonry Infill Walls, *Journal of Earthquake Engineering*, 1(4): 693–720.
31. Murty, CVR, and Jain, SK, 2000. Beneficial influence of masonry infills on seismic performance of RC frame buildings, *Proceedings, 12th World Conference on Earthquake Engineering*, New Zealand, Paper No. 1790.
32. Oropeza M, Michel C and Lestuzzi P (2010). A simplified analytical methodology for fragility curves estimation in existing buildings, 14<sup>th</sup> European Conference on Earthquake Engineering, Ohrid.

33. Özer B, Erberik MA (2008). Vulnerability of Turkish low-rise and midrise reinforced concrete frame structures, *Journal of Earthquake Engineering*, 12(2): 2-11.
34. Ramamoorthy SK, Gardoni P and Bracci JM (2006). Probabilistic Demand Models and Fragility Curves for Reinforced Concrete Frames, *Journal of Structural Engineering*, ASCE, 132(10): 1563–1572.
35. Seyed DM, Gehl P, Douglas J, Davenne L, Mezher N and Ghavamian S (2010). Development of Seismic Fragility Surfaces for Reinforced Concrete Buildings by Means of Nonlinear Time-history Analysis, *Earthquake Engineering and Structural Dynamics*, 39(1): 91–108.
36. Sheikh, MN (2005). Seismic Assessment of Buildings in Hong Kong with Special Emphasis on Displacement-Based Approaches, PhD Thesis, the University of Hong Kong.
37. Su RKL, Lee CL and Wang YP (2012). Seismic Spectral Acceleration Assessment of Masonry Infilled Reinforced Concrete Buildings by a Coefficient-based Method,” *Structural Engineering and Mechanics*, 41(4): 479–494.
38. Su RKL, Lee YY, Lee CL and Ho JCM (2011). Typical Collapse Modes of Confined Masonry Buildings under Strong Earthquake Loads, the *Open Construction and Building Technology Journal*, 5(Supp1 1-M2): 50–60.
39. Tsang HH, Su RKL, Lam NTK and Lo SH (2009). Rapid Assessment of Seismic Demands in Existing Buildings, the *Structural Design of Tall and Special Buildings*, 18(4): 427–439.
40. Vamvatsikos D and Cornell AC (2002). Incremental Dynamic Analysis, *Earthquake Engineering and Structural Dynamics*, 31(3): 491–514.
41. Zhu Y, Su RKL and Zhou FL (2007). Cursory Seismic Drift Assessment for Buildings in Moderate Seismicity Regions, *Earthquake Engineering and Engineering Vibration*, 6(1): 85–97.